NGU Rapport 92.330

Monitoring of Groundwater Flow with Electrical Resistivity at Haslemoen, Hedmark County

NORGES GEOLOGISKE UNDERSØKELSE

Postboks 3006 - Lade
7002 TRONDHEIM
Tlf. (07) 90 40 11
Telefax (07) 92 16 20

RAPPORT

Rapport nr. 92.330	ISSN 0800-3416	Gradering: Åpen

Tittel:

Monitoring of Groundwater Flow with Electrical Resistivity at Haslemoen, Hedmark County

Forfatter: M.Morris, N.O. Kitterød O.B. Lile J.S. Rønning	Oppdragsgiver: NGU / NVE / NTNF
Fylke: Hedmark	Kommune: Våler
Kartbladnavn (M=1:250.000) Hamar	Kartbladnr. og -navn (M=1:50.000) 2016 II Flisa
Forekomstens navn og koordinater: Haslemoen 6581 67272	Sidetall: 44 Pris: Kr. 65,- Kartbilag: 0

Feltarbeid utført:	Rapportdato:	Prosjektnr.:	Ansvarlig:
01.-04.05.91	08.01.93	63.2586.00	Jan S. Rønning

Sammendrag:

The purpose of this study was to investigate the possibility of using surface resistivity measurements to monitor the movement of an injected saltwater pulse. The experiment was conducted in the unconfined groundwater aquifer at Haslemoen. In the study area, the groundwater flows mainly towards the south with a velocity of approximately 0.2 m/day. The depth to groundwater level is approximately 2.5 m.

The experiment took place from May 1 to May 4, 1991. Saltwater was injected in the aquifer. The gradient and velocity of flow were artificially increased by continuous pumping from a well located 3 m northwest of the injection well. The "charged potential" (CP) configuration was used to monitor saltwater movement. The metal casing in the injection well served as the near electrode, and electrical potential difference was measured between electrodes placed in a radial array around the injection well.

Investigation of the change in potential as a function of time resulted in identification of the direction of groundwater movement. The effect of the pumping is seen clearly. The data also indicates that the direction of natural flow is locally towards the southeast. There appears to be a correlation between change in potential and velocity of groundwater flow.

This study confirms that surface resistivity measurements can be used to monitor groundwater flow. An advantage with using surface resisitivity measurements over convential tracer methods, is in the cost, as only one well for injection of the tracer is required.

Emneord:	Geofysikk	Hydrogeologi
Elektrisk måling	Grunnvannsstrøm	Løsavsetning
	Sporstoff	Fagrapport

Table of Contents

Figures:

1. Introduction

Studies have shown that surface resistivity measurements can be used to monitor groundwater flow (Bevc and Morrison 1991, Karous 1989, White 1990). The method involves injecting a tracer at a well and monitoring the tracer movement with surface electrodes. The advantage with this method over traditional tracer tests, is that only one well is required, greatly reducing cost.

The opportunity unexpectedly arose to test the method at Haslemoen in Hedmark County during a tracer test conducted by the Norwegian Water Resources and Energy Administration (NVE) (for location see figure 1). The purpose of the tracer test from NVE's standpoint was to optimize parameters for future tracer studies and not to conduct a geophysical experiment. Therefore, from a geophysical standpoint, the test was not optimum, however, as a test of the resistivity monitoring method, the results are useful.

2. Site description

In the study area, sediments were deposited in a narrow, northwest-southeast oriented, glacially eroded valley (Høye and Sand 1983). Deposition in the valley was largely controlled by the retreat of the Late Weichselian icecap in eastern Norway (Kitterød, et.al. 1992). In the test area, the sediment thickness is around 30 m. Interpretation of, among other things, georadar data collected in 1991 (Rønning and Mauring 1991), has resulted in a sedimentological model of the aquifer (Riis, in prep. 1992).

The sedimentary column has been divided into six stratigraphic units (Riis, in prep. 1992). For the purposes of this experiment, the important part of the sedimentary deposition is in the upper 10 m. This is dominated by sediments belonging to "Unit D". "Unit D" consists of medium-grained sand interpreted to have been deposited by a braided river system. The surface sediment, "Unit E", is a thin (less than 1m) silt layer overlying "Unit D". "Unit E" is interpreted to be an overbank deposit.

At the time and location of the experiment, the depth to groundwater level was approximately 2.5 m. The groundwater level drops to the south in the area with a gradient of approximately 3m/km. Permeability of the aquifer in the test area ranges from around 1.1×10^{-2} cm/s to 5.8×10^{-2} cm/s (Nordal, 1986). Natural velocity of groundwater movement is approximately 0.2 m/day.

3. Method

The "charged potential" (CP) or "mise-à-la-masse" method in ore prospecting was used to monitor saltwater movement. In this method, current is sent between two electrodes, one of which (the near electrode) is embedded in the conductive zone (injection well), while the other (the far electrode) is placed a large distance (approximately infinite) distance away. The influence of the far electrode in the measurement area is negligible. The potential difference is measured between two electrodes which are moved about systematically in an array around the near current electrode (gradient measurements). The potential difference is related to apparent resistivity by the equation:

$$\Delta V = \frac{\rho_a * I(r_2 - r_1)}{2\pi * r_2 r_1} \tag{1}$$

where ΔV is the potential difference measured between two electrodes, ρ_a is the apparent resistivity, **I** is the current, and $\mathbf{r_1}$ and $\mathbf{r_2}$ are distances from the potential electrodes to the embedded near current electrode.

The current sent between the near and far electrodes will preferentially seek out areas of high conductivity (low resistivity). Thus, the current density is higher in the part of the formation containing saltwater. The measured potential difference is related to current density by Ohm's law:

$$\Delta V = j\rho d \tag{2}$$

where j is the current density, ρ is the formation resistivity, and d is the spacing between potential electrodes. The measured potential difference decreases as the current is drawn into areas of higher saltwater concentration. Apparent resistivity calculated from equation (1) thus also decreases.

4. Procedure

Saltwater was chosen as the tracer. The experiment took place from May 1 to May 5, 1991, while the ground surface was still wet from melting snow. Twelve kg of salt mixed with 700 liters of fresh water were injected at a depth of approximately 3 m within a one-hour period. Conductivity of the injected water was 46.2 mS/cm. Because the formation has such low porosity, pumping was commenced 3.5 hours prior to injection at a well located 3 m northwest of the injection well. Pumping was sustained throughout the experiment, starting with 70 l/min and lowering to

55 l/min at the end of the experiment (figure 2). Conductivity of the pumped water and pumping rate were recorded at frequent intervals. The output water from pumping was released into an open ditch 18 m south of the injection well.

Monopolar 200 mA square current pulses were used for all measurements. Current "on-time" was 2 seconds while "off-time" was 6 seconds. The far electrode was located 1000 m north of the near electrode. The metal casing in the injection well served as the near electrode. Prior to each time measurement, the potential grid was levelled to "infinity" to an electrode located 450 m southwest of the near current electrode.

Measurements of potential were made on a radial array in eight directions with stations at 1, 2, 4, 8, 12, 16, 20 and 30 meters from injection well. Two non-polarizing electrodes ($Cu/CuSO_4$) were used and moved continuously about the array, with the locations kept as constant as possible. Possible self-potential field was compensated before reading the effect of current pulses. Potential data was collected eight times. Each time measurement corresponds to a certain "CP" number (table 1). Thus, CP0 refers to the initial pre-injection measurement, while CP5 was recorded starting 41 hours after injection. It took approximately one hour to measure the potential values for the entire array.

Table 1. Measurements with the "CP" method.

CP #	Date	Time	Hrs. after inj.
CP0	1.5.91		
CP1	1.5.91	15:15-16:15	0-1
CP2	1.5.91	18:15-19:15	3-4
CP3	2.5.91	08:15-09:15	17-18
CP4	2.5.91	18:00-19:00	26.75-27.75
CP5	3.5.91	08:15-09:15	41-42
CP6	3.5.91	18:15-19:15	51-52
CP7	4.5.91	10:00-11:00	66.75-67.75

5. Results and Discussion

5.1. Measurements

The initial time measurement (CP0) could not be used, because the current was not measured correctly. Therefore, there is no true "baseline" data with which to normalize post-injection values.

The measured potential difference values were summed along each "arm" of the radial array for all time intervals. In figures 3-6, examples of these potential curves are shown. For clarity, only three time intervals are plotted. The information required to describe the saltwater movement is all contained in this data. The potential decreases from CP1 to CP3 time, and increases from CP3 to CP7 time, except to the north, northwest, and west, where there is an anomalous effect. However, in order to interpret the distribution of potential, and thus the saltwater, in space and time, it is advantageous to present the data in a different manner.

The minimum value of potential difference occurs 3 to 27 hours after injection (from CP2 to CP4 measurements). This is evidenced by the plots of potential difference vs. time (figure 7-14). The minimum value of potential difference is a result of the potential dropping as saltwater moves into the formation. As the saltwater is pumped out and the formation water returns to its' original composition, the potential difference values increase.

5.2. Sources of error

The potential measured at the end of each radial arm, was plotted to show the change with time (figure 15). With a small scale experiment such as this, the effect of saltwater 30 m away from the injection well was expected to be very low. (Figures 7 to 14 support this. Note that the ordinate scale in figure 15 is more detailed than that in figures 7 to 14.) Using CP1 time as a reference, the maximum change in potential is 48 mV, or 3%, in the northeast direction. At times later than CP2 measurements, the potential increases in general with time, reflecting the change in weather with the ground drying and becoming more resistive. Variations in radial direction are expected to be caused by variations in the drying process due to differences in vegetation. From this, we can conclude that the effect of the ground drying does not influence the results seriously.

The curves of potential difference vs. time (figures 7-14) appear to stabilize by the CP6 measurement for most station intervals. The change in potential difference is small in the time interval CP6 to CP7, indicating a return of the formation water to its' original composition (values for two directions are listed in table 2). The range of values of percent change for far stations and later times indicate that variance is due to environmental changes.

Table 2. Percent change in potential difference from preceding time measurement.

Station int.	CP2	CP3	CP4	CP5	CP6	CP7
NW 1-2	-28	-32	88	39	4	6
SE 1-2	-23	-6	42	4	13	4
NW 2-4	-21	13	51	33	0	10
SE 2-4	-19	-6	41	20	-4	-9
NW 4-8	-15	36	-4	12	2	7
SE 4-8	-21	-2	30	24	10	25
NW 8-12	-13	33	-3	-1	12	5
SE 8-12	-19	-4	28	17	-5	17
NW 12-16	-8	25	-2	7	0	3
SE 12-16	-19	-7	25	16	9	2
NW 16-20	-10	25	0	5	1	5
SE 16-20	-15	-10	20	13	5	2
NW 20-30	-9	20	0	2	2	3
SE 20-30	-12	-3	19	3	4	0

Considerable error arises in measurement of potential difference when the potential electrodes are not positioned correctly (table 3). This is especially true for the near station interval, 2-1. A misplacement of 5 cm of one of the potential electrodes results in a 11% error in measurement. Comparing this error with the change in potential difference with time (table 2), it is clear that electrode placement is of great importance. In this experiment, due to good marking of measuring points on the ground, the misplacement is less than ±0.01 m. Thus the error due to electrode misplacement is less than 2%.

Table 3. Error resulting from electrode misplacement.

Station int.	Mispl., cm	% error
1-2	1	2
	3	6
	5	11
	10	22
2-4	1	1
	3	3
	5	5
	10	11
4-8	1	<1
	3	2
	5	3
	10	5
30-20	1	<1
	3	<1
	5	1
	10	2

Discharge of the pumped water 18 m south of the injection well influences the measured potential and is a source of error in interpretation.

5.3. Determining groundwater flow velocity

It is evident from the potential difference curves (figures 7-14) that the chosen time sampling interval was not short enough to detect the maximum invasion of saltwater into the formation. This is confirmed by comparing values of calculated apparent conductivity from equation (1) (apparent conductivity = $1/\rho_a$) with measured conductivity of the pumped water (figures 16-19). The values are not expected to match exactly, since apparent conductivity is a bulk measurement which includes formation and pore fluid conductivity, and is averaged over a large, inhomogeneous area. Conductivity of pumped water show a maximum conductivity value 7 hrs. and 40 min. (between CP2 and CP3 time) after saltwater injection. The greatest decrease in potential value should occur some time before that, when the conductivity of the formation water is at a maximum. However, the frequency of potential measurements was not high enough to detect the greatest decrease. Nevertheless, the conductivity curves (apparent and measured) have similar trends, which indicates that if the measuring frequency is high enough, the CP method can be used to calculate the velocity of the salt pulse in the sediments. This is in agreement with earlier investigations (Karous 1989).

5.4. Establishing "background" values

Conductivity of the pumped water had returned to within 6% of the preinjection value by CP6 time, indicating that the values have stabilized. This is also what the apparent conductivity curves are indicating. Therefore, CP7 potential values were chosen as reference or "background" values, with which earlier measurements could be normalized. The assumption is then, that by CP7 time, the saltwater was essentially out of the system, and the formation water had returned to its original composition. CP7 values are the best replacement for CP0 values, which could not be used.

5.5. Determining groundwater flow directions

The change in potential with respect to background (CP7) as a function of time was computed and plotted for four time intervals (figures 20-23). There is a decrease in potential for all station intervals from CP1 to CP2 as a result of the saltwater moving into the formation (figure 20). The near station intervals, 2-1 and 4-2, appear to be influenced by pumping for this time interval. The largest decrease for these two station intervals occurs from the west to the north, in the direction of artificially provoked flow. For station intervals farther away, the largest decrease in potential occurs to the south and southeast. The high negative value in the southerly direction can be at least partly explained by the ditch located approximately 18m south of the injection well, where pumped water was discharged. The potential decrease to the south thus reflects the increasing conductivity of the ditch water. The potential decrease to the southeast is interpreted to be indicative of the natural direction of groundwater flow.

For the interval CP2 to CP3 (figure 21), the maximum decrease in potential for station intervals 2-1 and 4-2 occurs to the northwest and north. For the station intervals farther away, the maximum decrease is to the south and southeast. Again, this indicates that a portion of the saltwater has moved in the direction of natural groundwater flow to the southeast. It appears that discharge of water into the ditch is still influencing the measurements to the south. The strong positive change in westerly and northerly directions for station intervals farther away is a result of the saltwater being pumped out, and the resistivity (and potential) increasing.

The positive change for the intervals CP3 to CP4 and CP4 to CP5 (figures 22 and 23) are a result of the saltwater being pumped out and the formation water returning to its' preinjection composition. The higher values for the near stations, especially to the north and northwest indicate that most of the flow is forced to occur in these directions. However, it is also evident that the greatest positive change occurs otherwise from the east to the south. This reinforces the interpretation of the natural direction of groundwater flow to the southeast, in the direction of the greatest dispersion of the salt. In these time intervals, the ditch does not appear to have great influence.

The normalized potential difference values were plotted on a map and hand-contoured (figures 24-29). Hand-contouring was necessary because of the variation in measuring point density. The effect of saltwater in the groundwater is shown as a percentage of background values (CP7 data). The maximum effect drops from 70% at CP1 time to 45% at CP3 time, after which it increases to 90% at CP5 time and drops back to 80% at CP6 time. This is a result of the formation being most conductive at CP3 time, after which it gradually returns to its' original state.

The drop in effect from 90% at CP5 time to 80% at CP6 time has not been explained. It does not seem to be due to a random decrease in potential as evidenced by the ΔCP6/ΔCP7 map. Rather there is a trend to the southeast. A possible explanation is that the saltwater plume is optimally located for the CP6 measurements, but not for the CP5 measurements.Another explanation lies possibly in the fact that CP7 data cannot really be considered background.

A high percentage anomaly to the south centring around 18m is prevalent on the ΔCP1/ΔCP7 to ΔCP3/ΔCP7 maps. This is due to the pumped water being poured into a ditch 18m to the south. The background conductivity in the ditch area is greater for the first measurement (CP1). Background conductivity is lower for the following measurements, but this area is still anomalous due to the discharge of pumped water.

The ΔCP3/ΔCP7 map shows a maximum effect between injection and pumping well indicating a displacement of salt water in this direction. A steep gradient to the northwest of the pumping well indicates that very little salt water is moving into this area due to artificial barrier created by pumping. The shape of the contours with elongations to the south and southeast indicate the natural direction of groundwater flow.

The anomaly 2m southeast of the injection well is interpreted to be a local barrier to groundwater flow. The high percentage value indicates that the potential difference is not changing with respect to background. In other words, the conductivity is not changing; little saltwater is moving into or out of this area.

6. Suggestions for further work

There seems to be a correlation between the potential measurements and the velocity of the saltwater pulse. White (1988) used resistivity measurements of a saltwater injection experiment to estimate groundwater velocities. Time and distance to the maximum resistivity decrease are used in the calculation. The velocity estimate thus obtained is a bulk velocity, representative of a larger volume of the aquifer than that obtained by traditional tracer methods.

With access to a three dimensional modelling program, the movement of saltwater and resulting effect on electrical potential could be modeled. This has been done in a study by Bevc and Morrison (1991), in which they showed that the groundwater flow was in a different direction than that predicted by well measurements. The density and placements of wells was not adequate to detect the main direction of movement.

In an experiment described by Williams, et.al. (1990), steady-state recharge conditions were established prior to injecting the saltwater pulse. The steady-state recharge was maintained throughout the experiment. This is preferable to our procedure of pumping at a location away from the injection well. Flow is enhanced, but it occurs in natural directions. Also, only one well is required.

7. Conclusion

This study has shown that surface resistivity measurements can be used to monitor groundwater movement. The main, artificial direction of flow towards the northwest was recognized. From the data it was also possible to determine the natural direction of groundwater flow. In this area, the natural flow direction is interpreted to be towards the southeast. The method seems to be able to tell us the groundwater flow velocity.

In future experiments, it is important to obtain accurate pre-injection values of potential. These should preferably be measured several times, over a period of days, in order to remove effects of changing weather, and to ensure repeatability.

The sampling interval in time should have been smaller in order to adequately monitor the saltwater movement. To achieve a smaller sampling interval, and to avoid errors arising from misplacing electrodes, a multi-electrode system with automated sampling is recommended (Williams 1990).

8. References

Bevc, D., Morrison, H.F., 1991. Borehole-to-surface electrical resistivity monitoring of a saltwater injection experiment. *Geophysics, 56, 769-777.*

Høye, T., Sand, M., 1983. Geofysiske undersøkelser av kvartære sedimenter ved Haslemoen og Flisa, Hedmark. *M.Sc. thesis, University of Oslo.*

Karous, M., 1989. Geoelektrické metody průzkumu. Praha, *SNTL - Nakladatelství tecknické literatury*

Kitterød, N.O., et.al., 1992. Haslemoen - project - main results and experience - report to the NTNF/BBV program.

Nordal, O., 1968. Grunnvannsbalanse - en modellstudie fra Haslemoen. *M.Sc. thesis, Norwegian Agricultural University.*

Riis, V., in prep. 1992. Hydrogeologi og avsetningsmodell av Haslemoen. *M.Sc. thesis, University of Oslo.*

Rønning, J.S., Mauring, E., 1991. Georadar og refleksjonsseismiske målinger på Haslemoen. *NGU report nr. 91.270,* ISSN 0800-3416.

White, P.A., 1988. Measurement of ground-water parameters using salt-water injection and surface resistivity. *Ground Water, 26, 179-186.*

Williams, G.M., Jackson, P.D., Ward, R.S., Sen, M.A., Lovell, M., Meldrum, P., 1990. Determinations of formation heterogeneity at a range of scales using novel multi-electrode resistivity scanning techniques. *NEA Workshop on Flow Heterogeneity and Site Evaluation, Paris, France, 22.-24. October, 1990.*

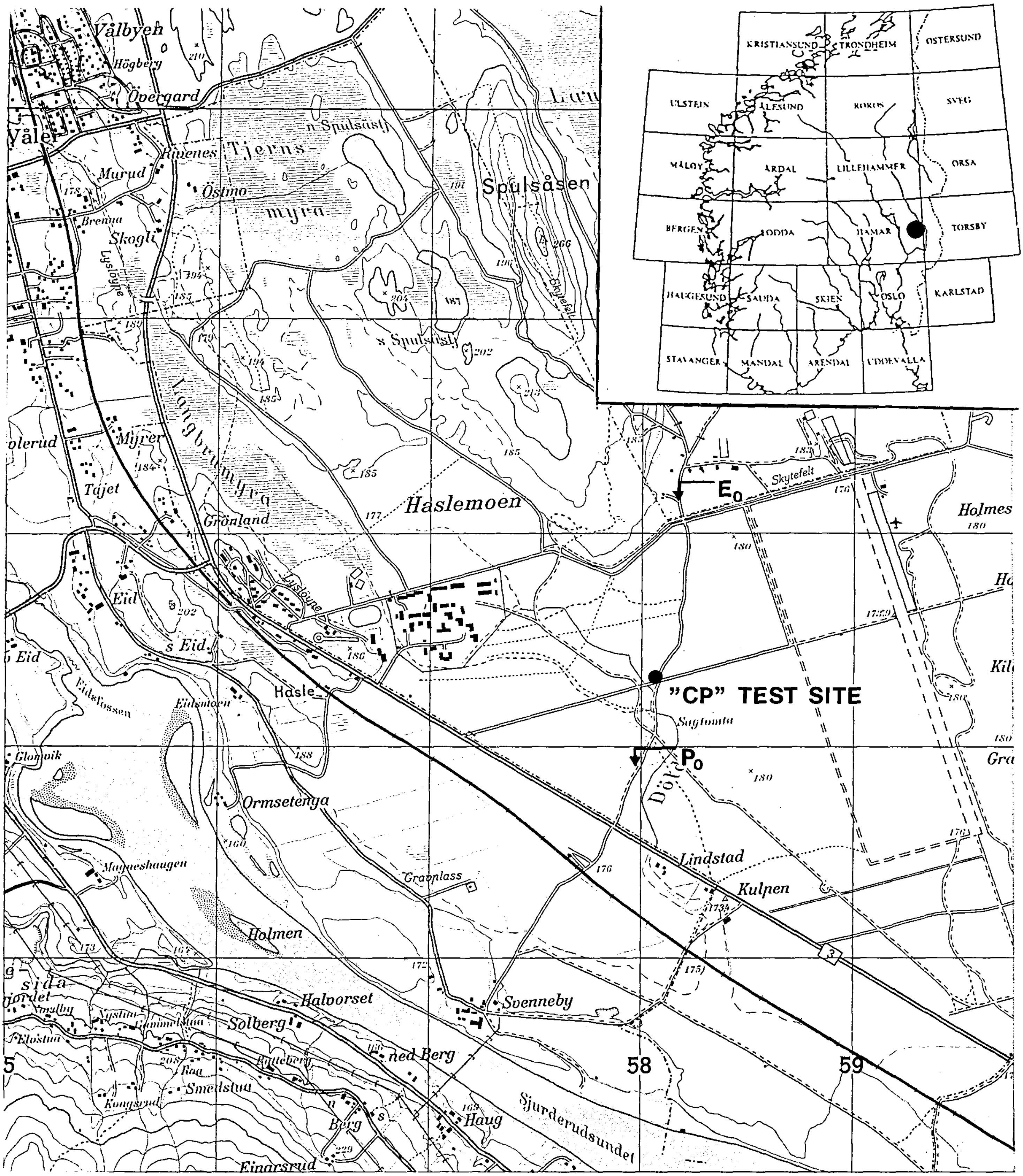

Figure 1. Test site and electrode location.

E_0 "far away" current electrode
P_0 "far away" potential electrode
SCALE 1: 25 000

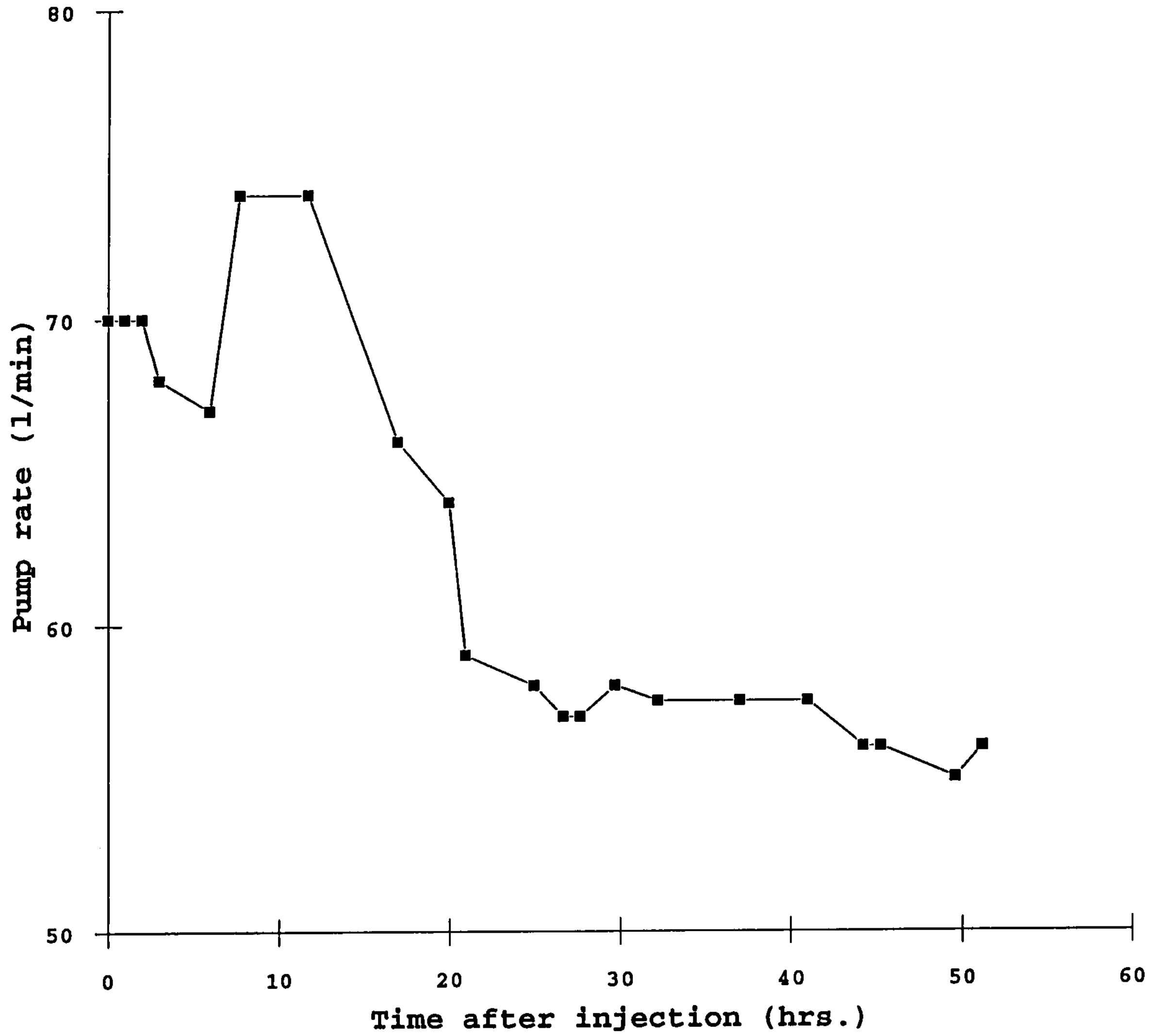

Figure 2. Rate of pumping during experiment.

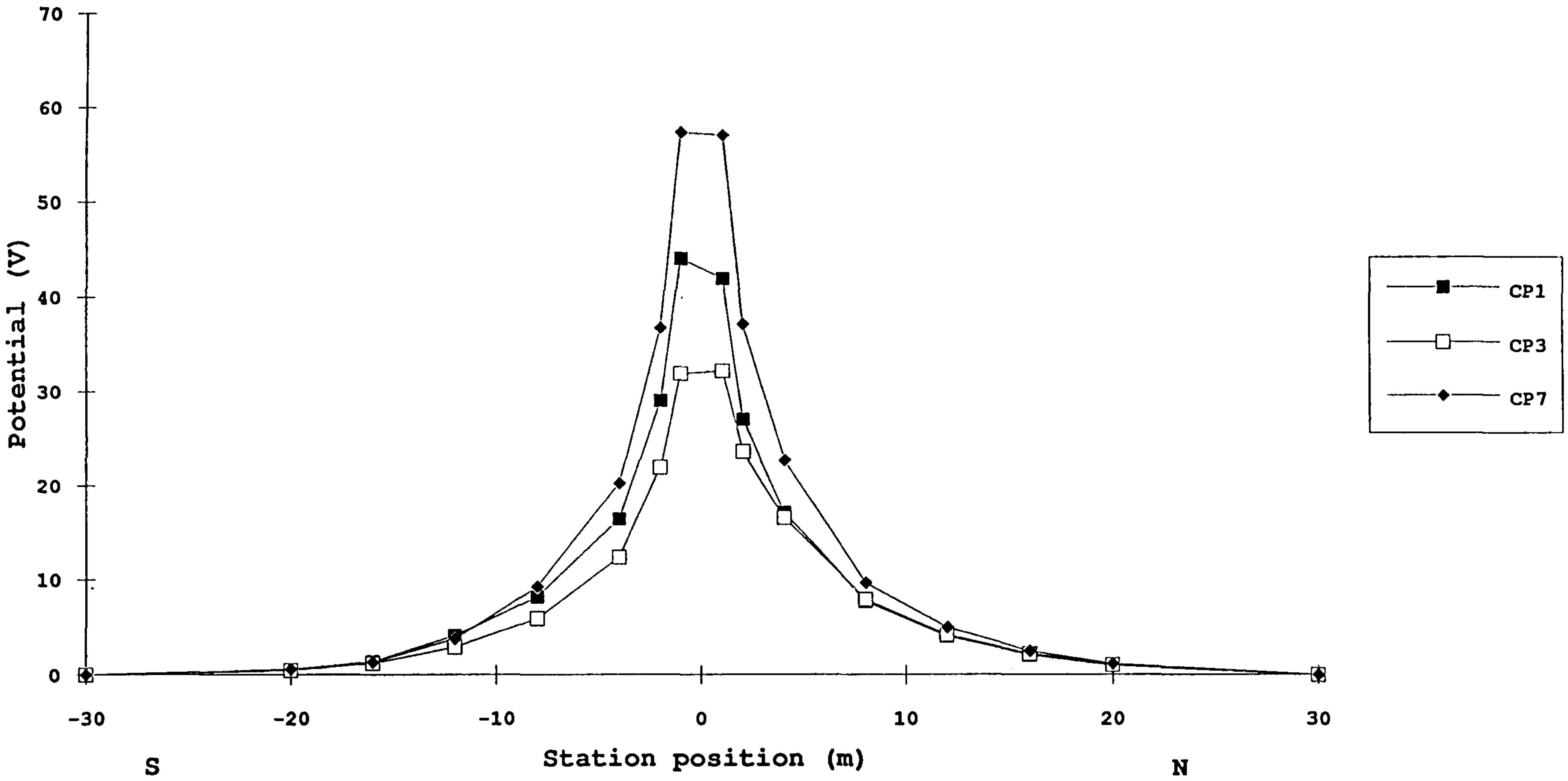

Figure 3. South - North potential

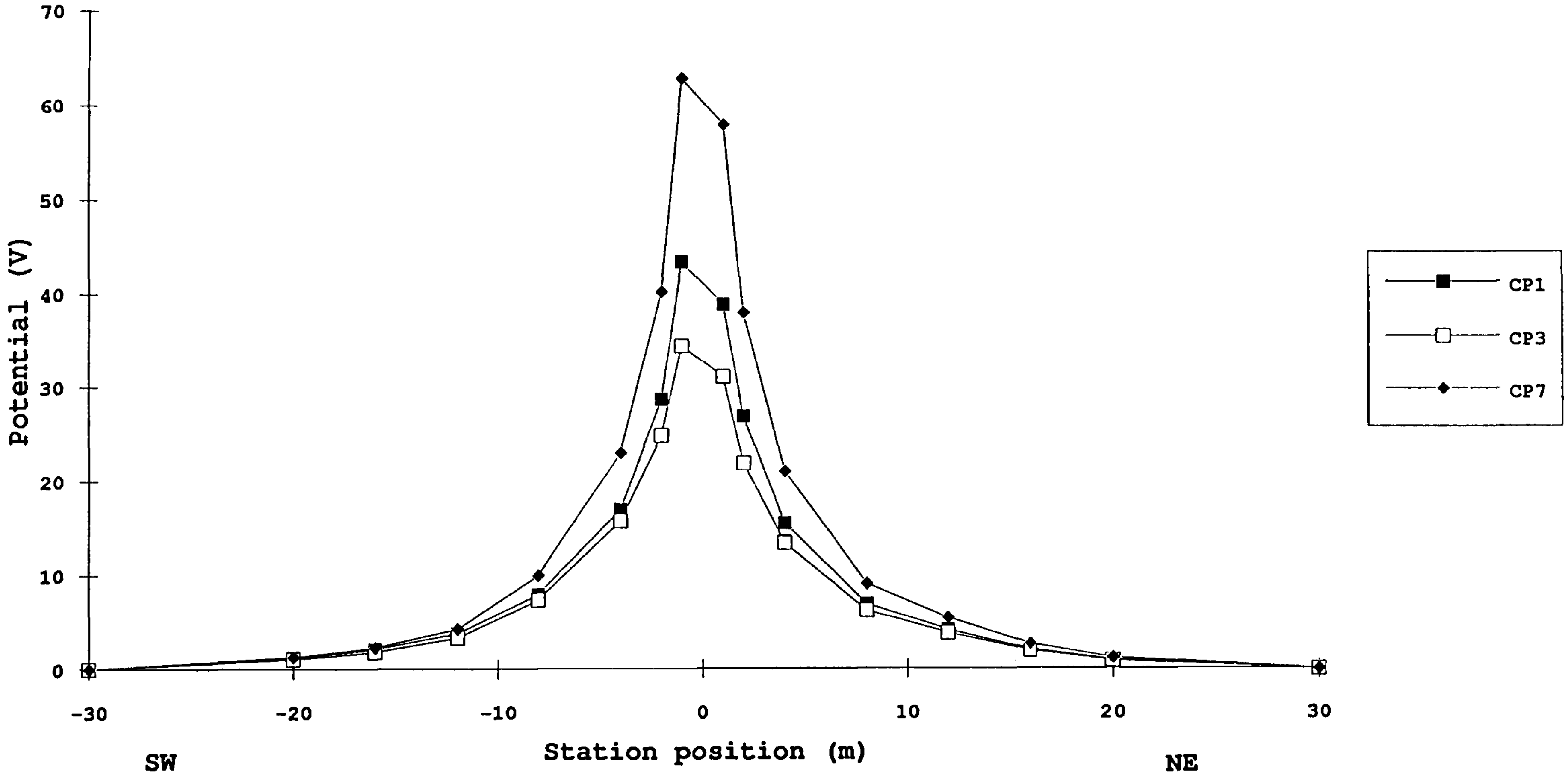

Figure 4. Southwest - Northeast potential

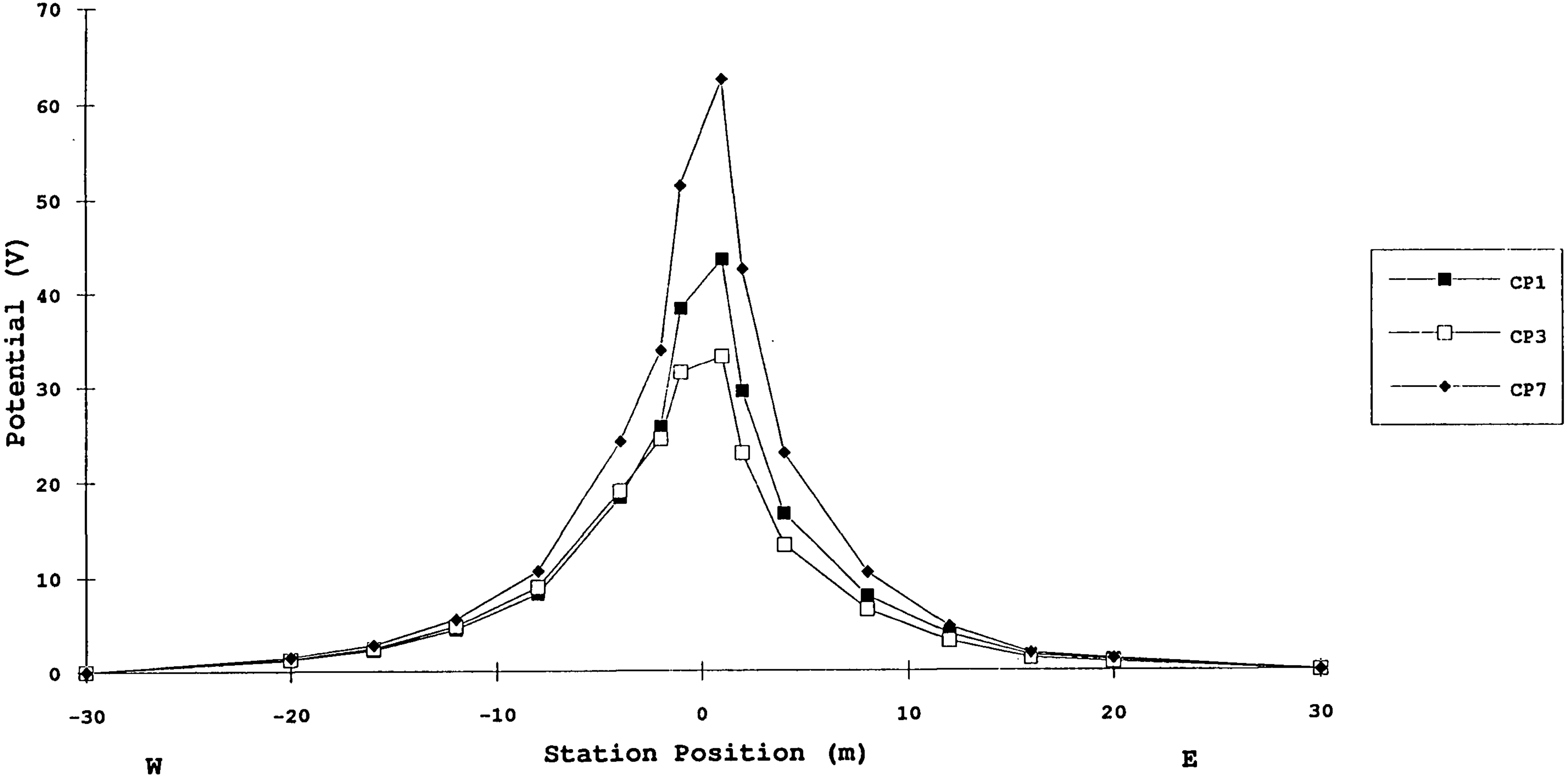

Figure 5. West - East potential

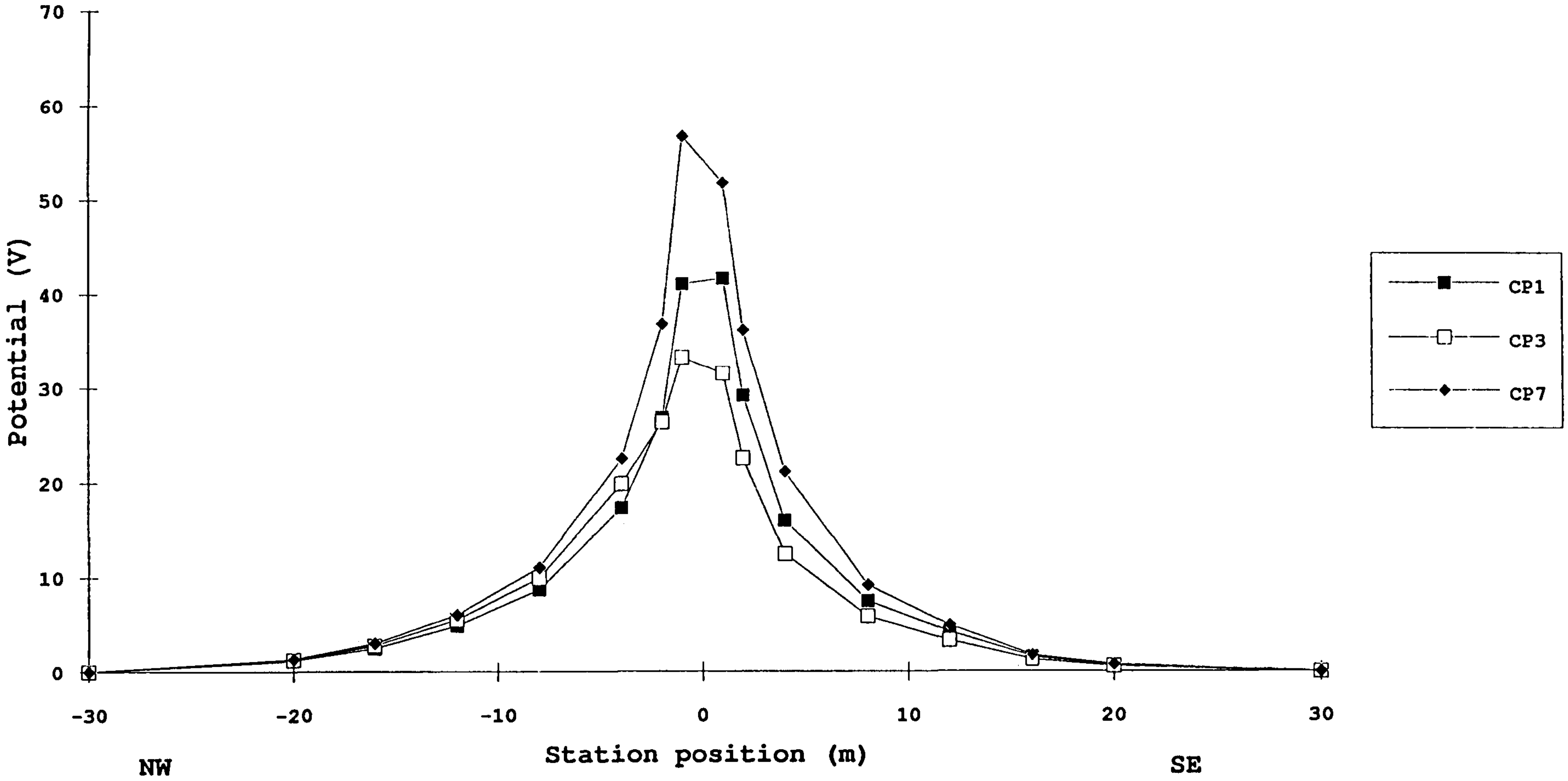

Figure 6. Northwest - Southeast potential

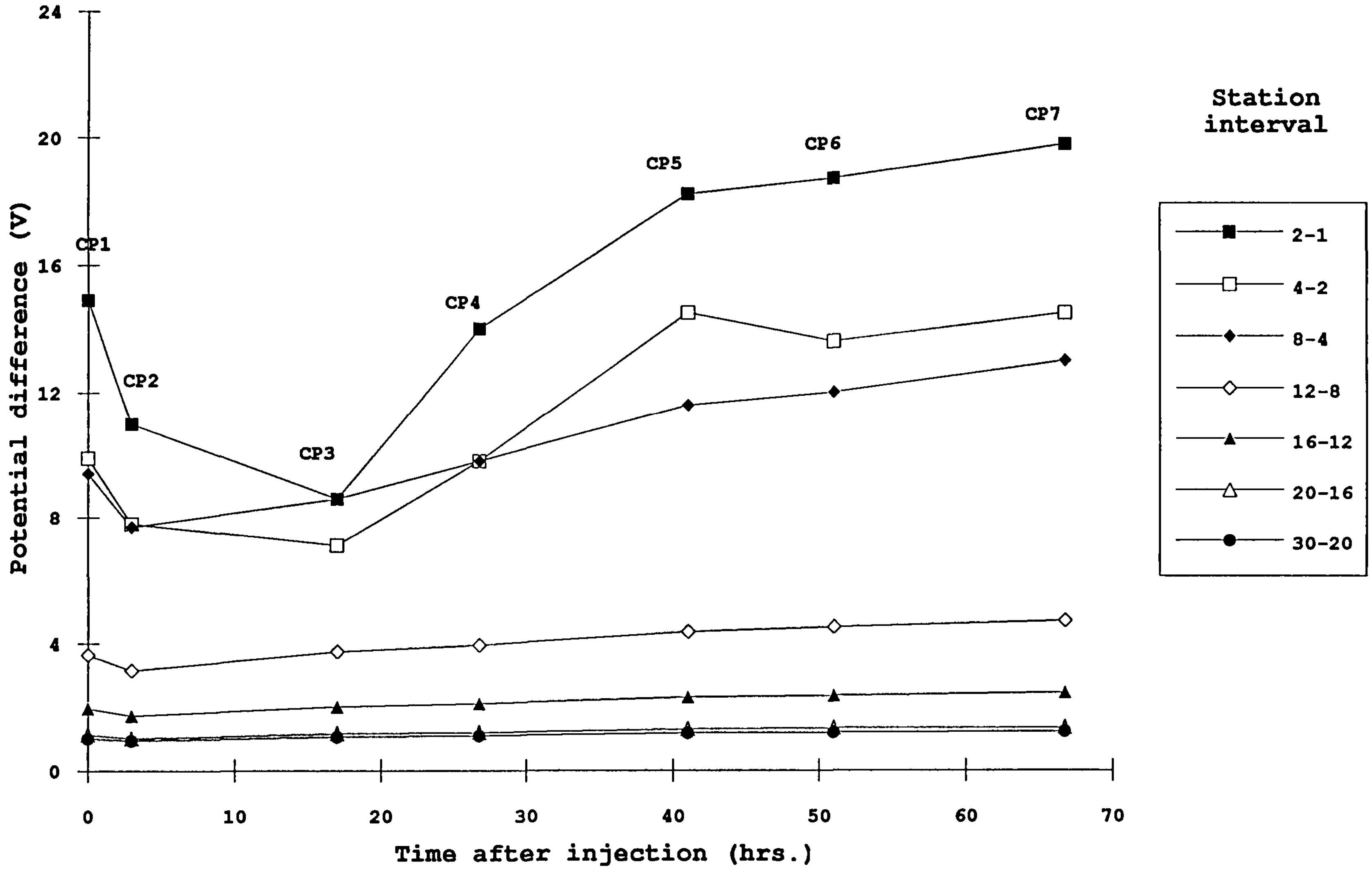

Figure 7. Potential difference between stations to the north

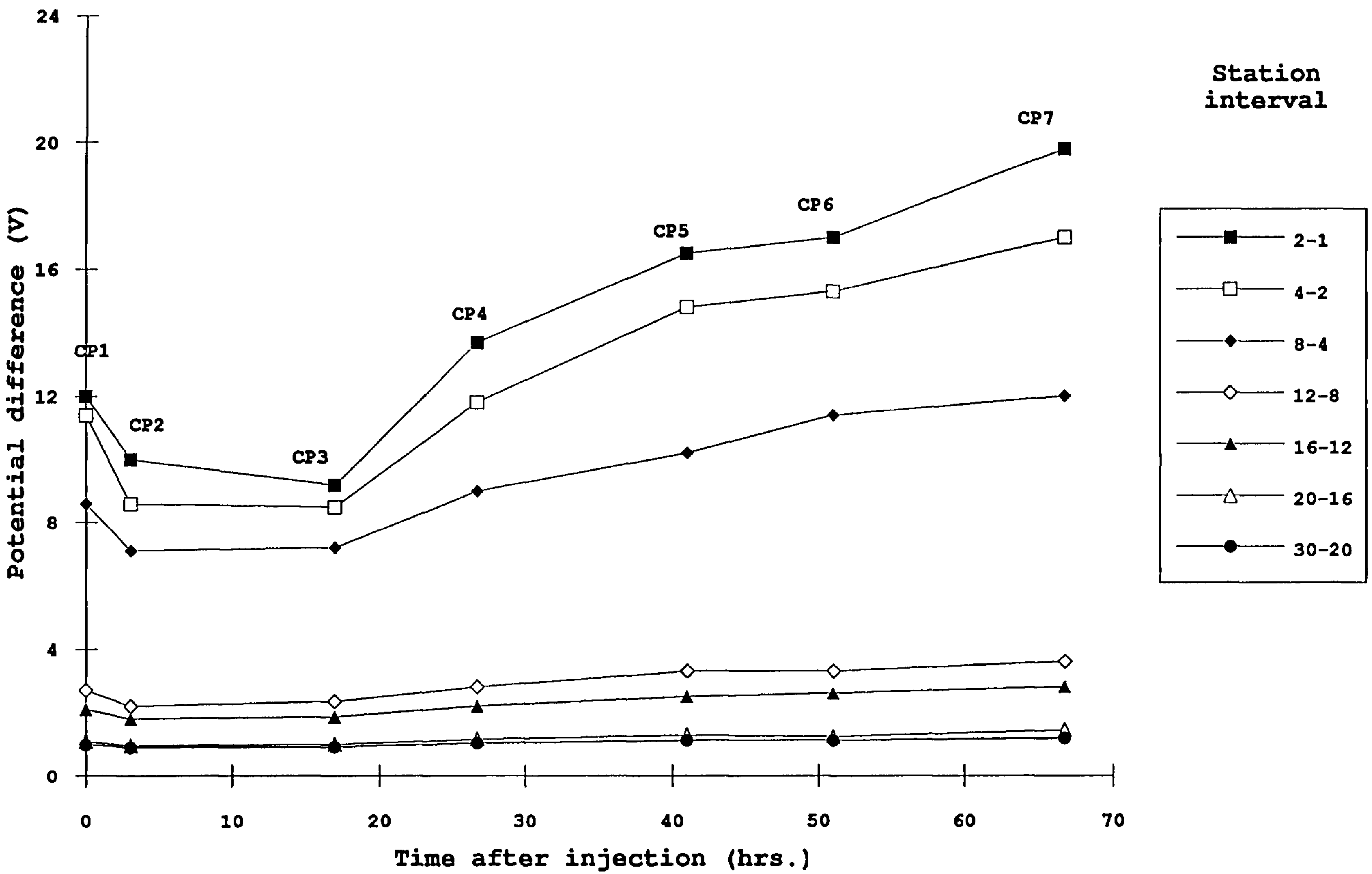

Figure 8. Potential difference between stations to the northeast.

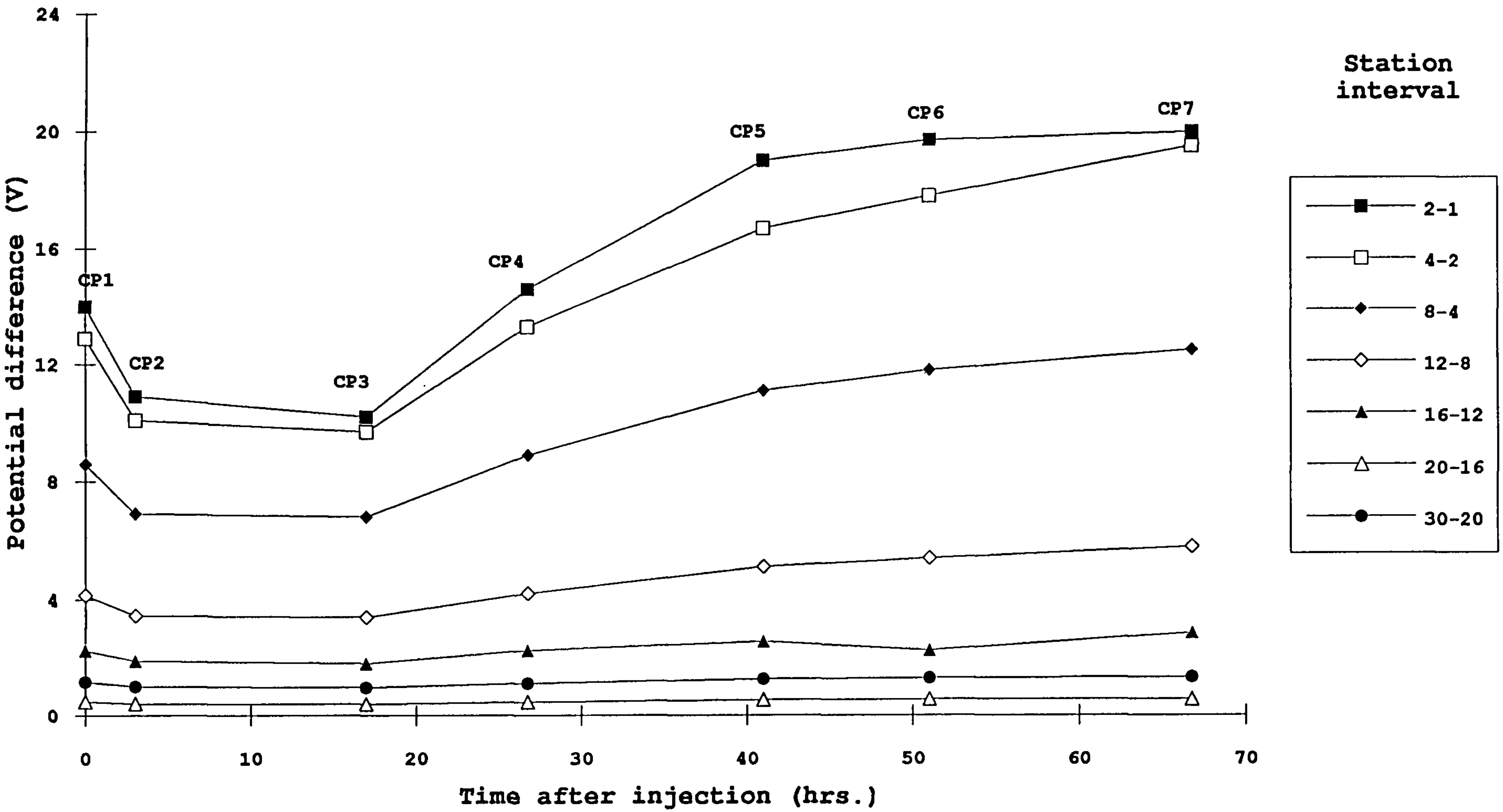

Figure 9. Potential difference between stations to the east.

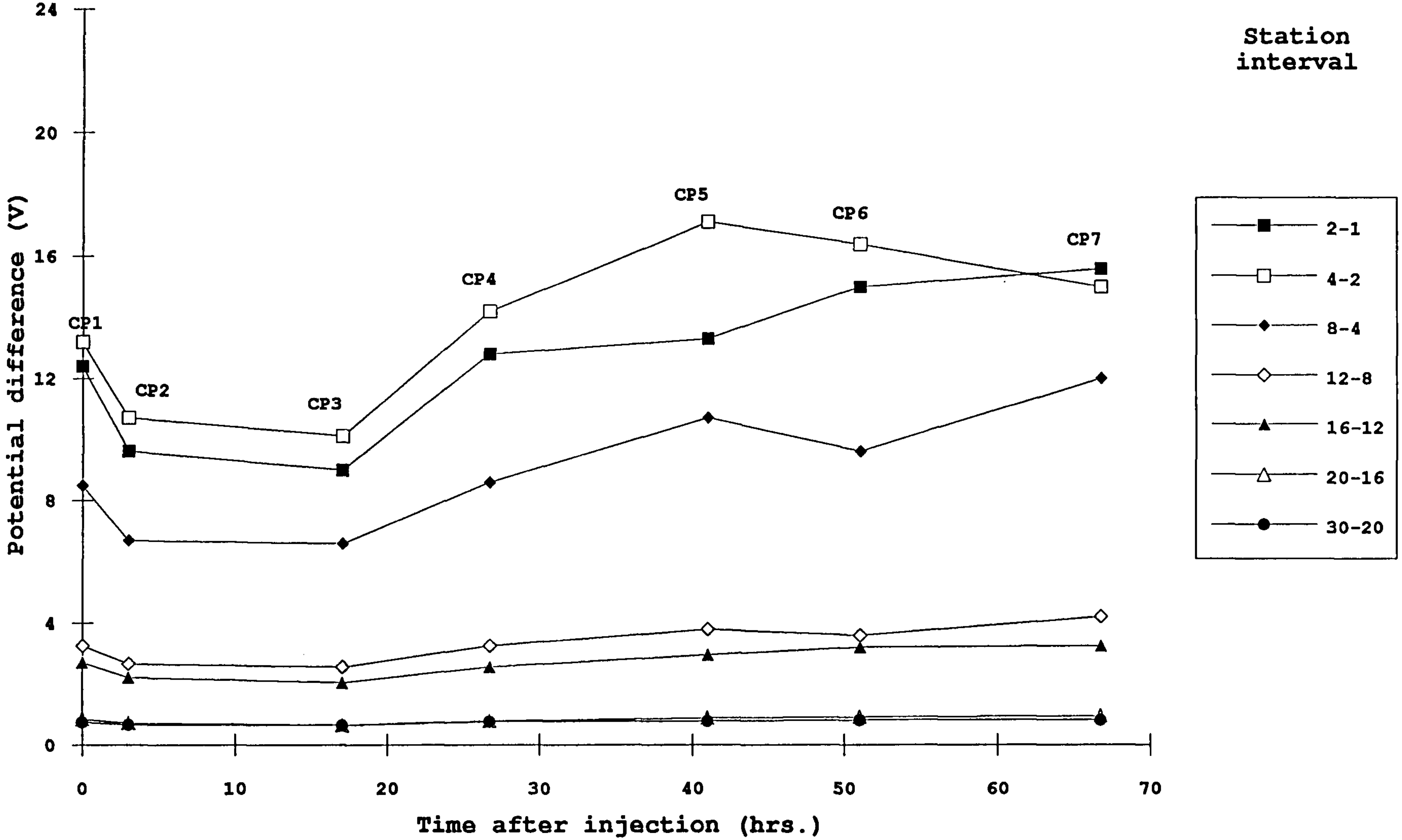

Figure 10. Potential difference between stations to the southeast.

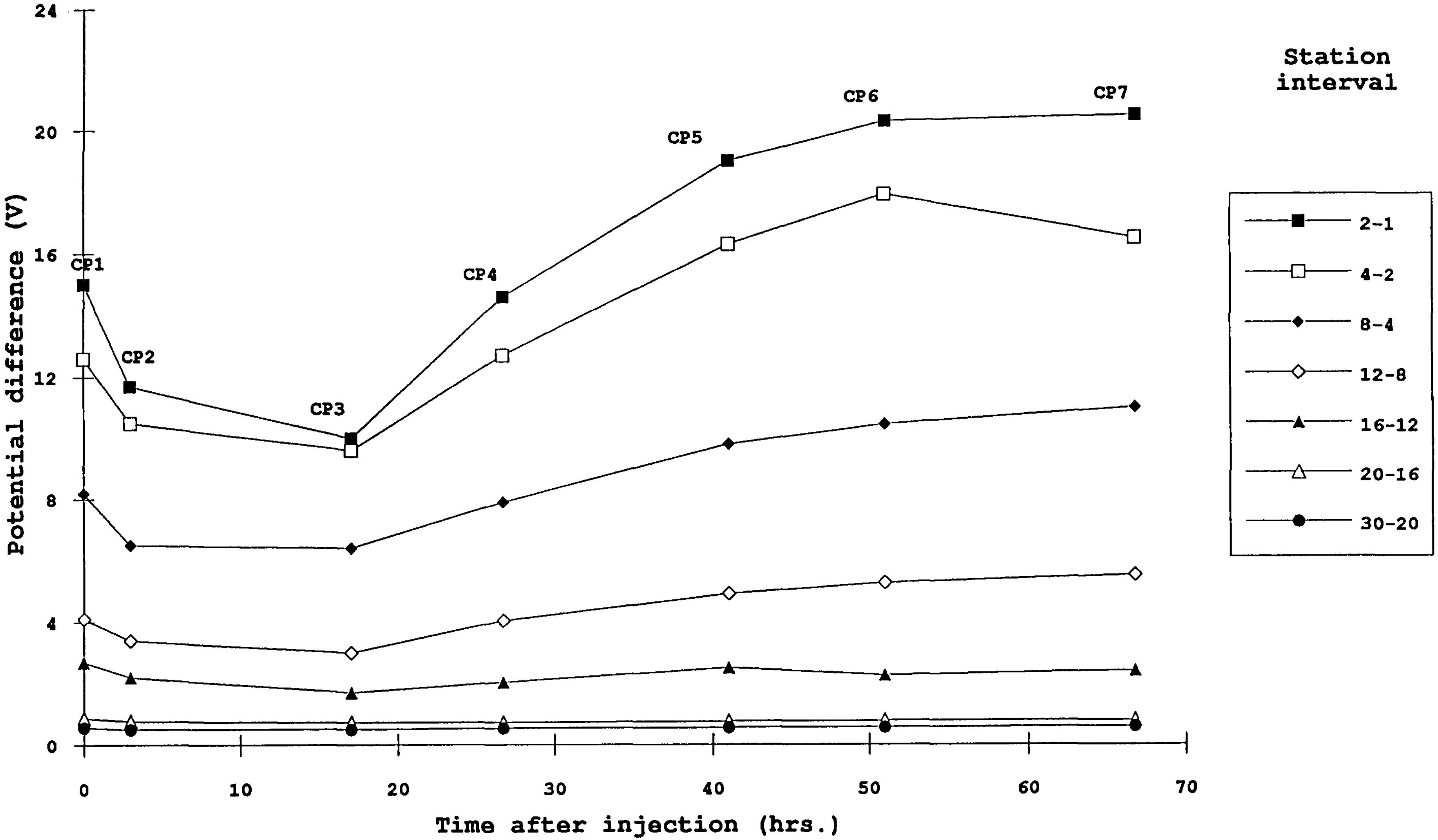

Figure 11. Potential difference between stations to the south.

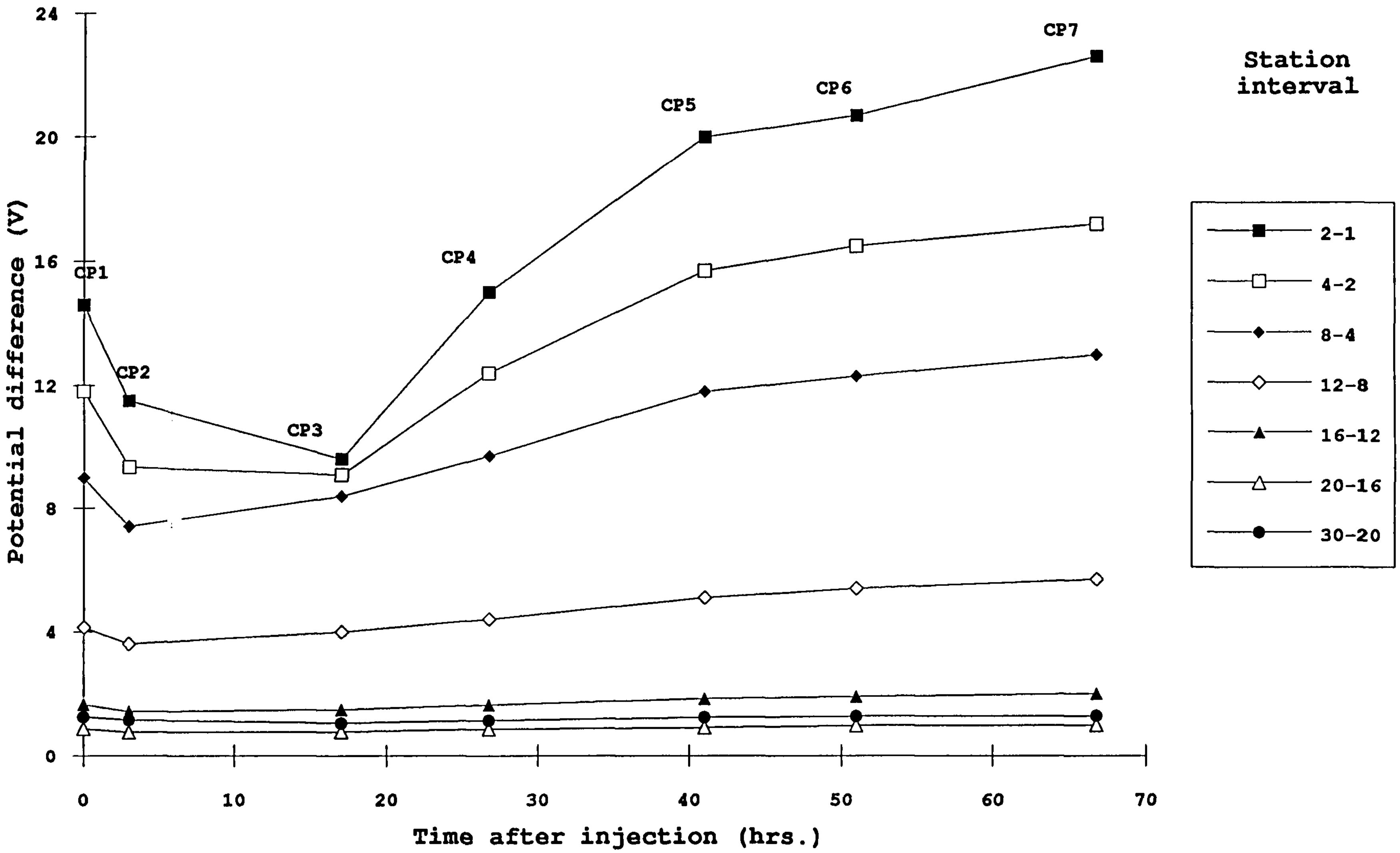

Figure 12. Potential difference between stations to the southwest.

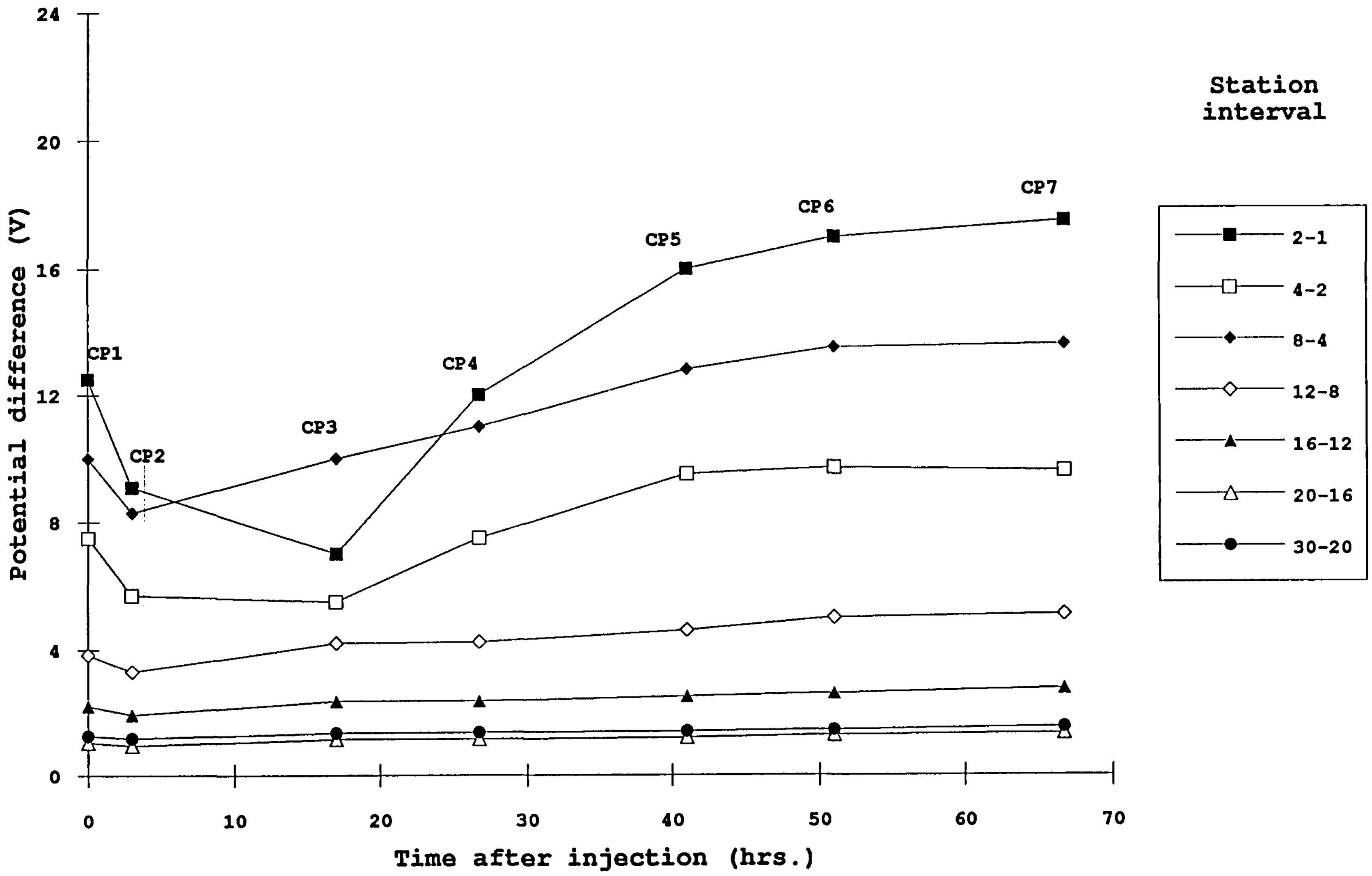

Figure 13. Potential difference between stations to the west.

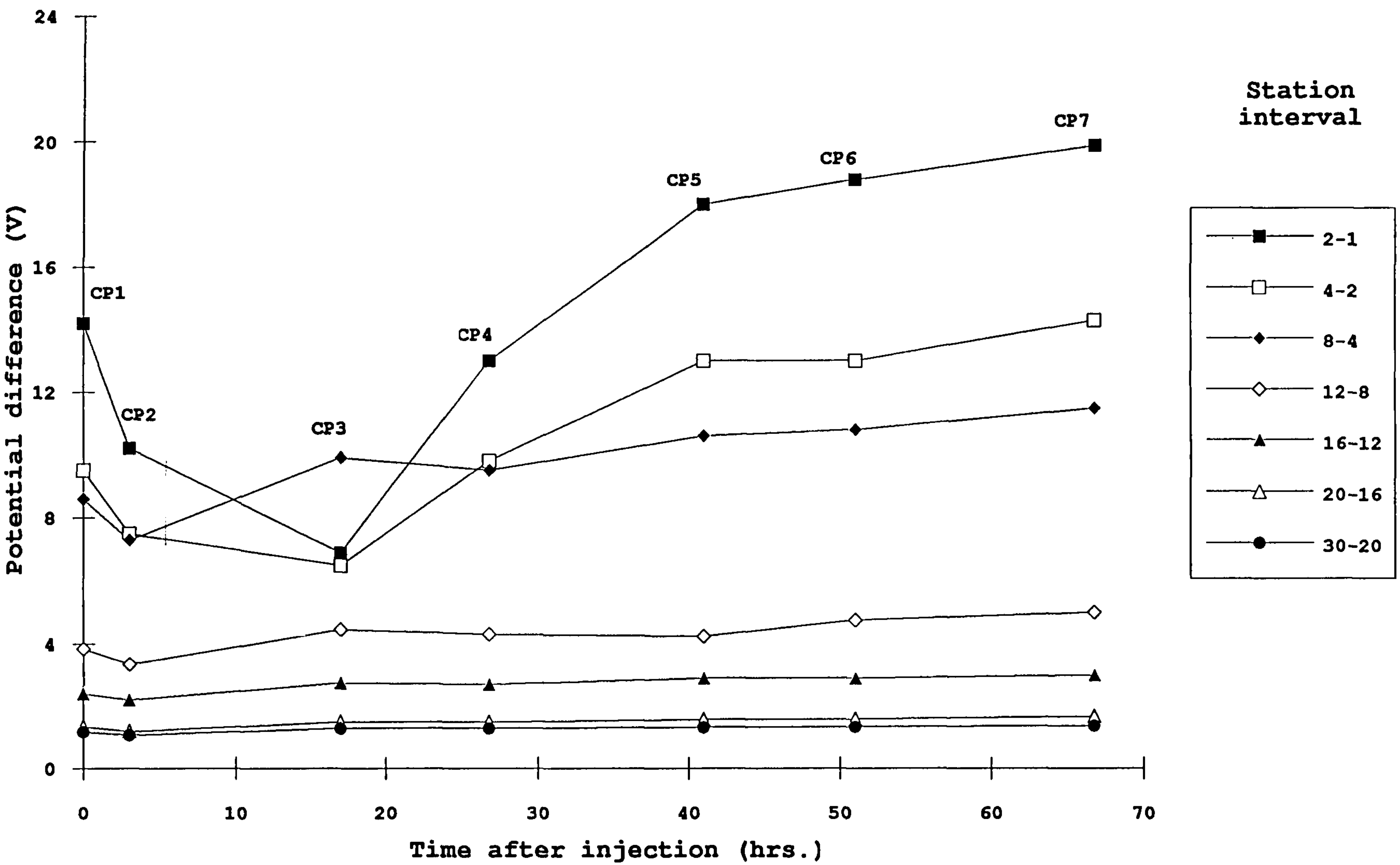

Figure 14. Potential difference between stations to the northwest.

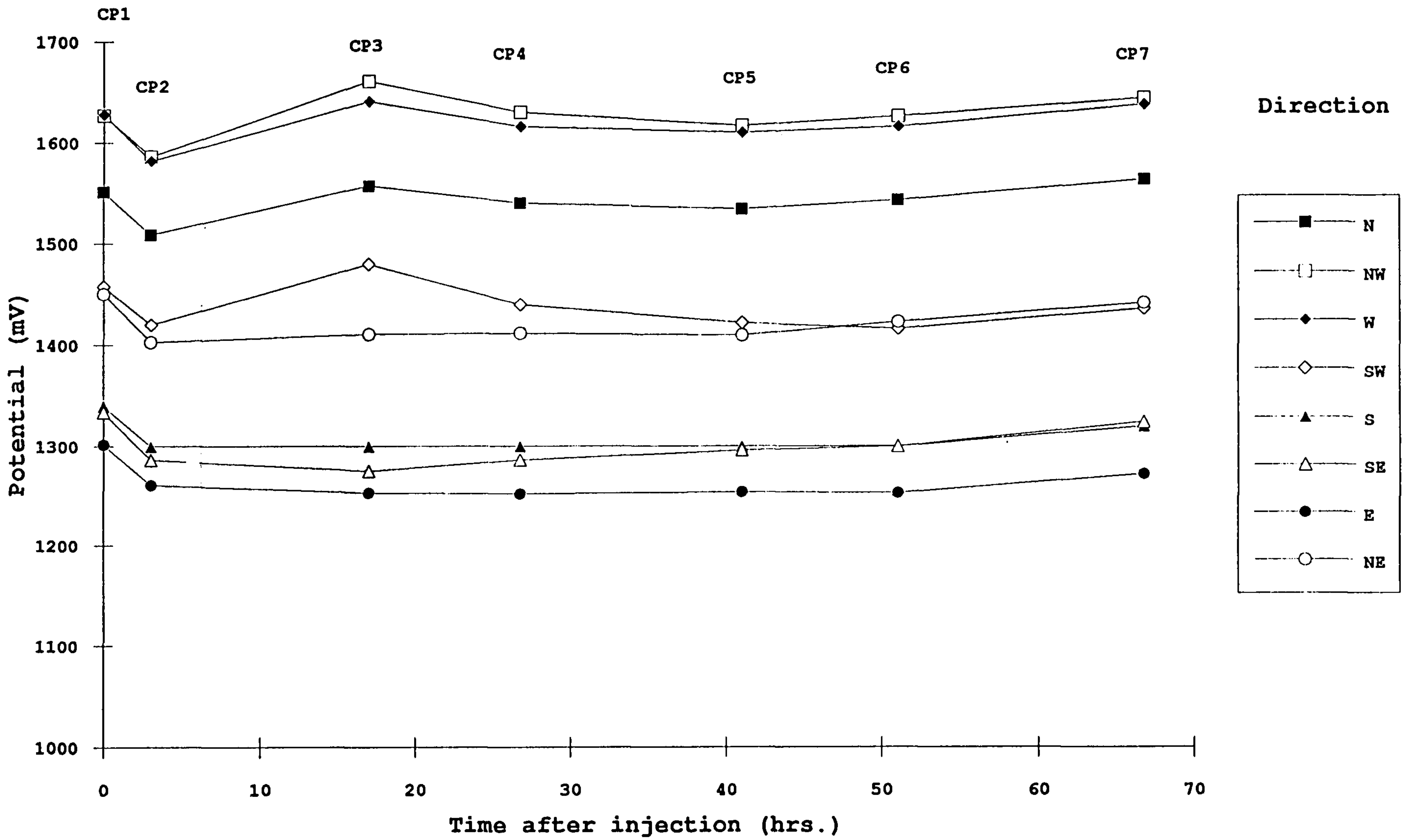

Figure 15. Potential calculated at the end of each array arm.

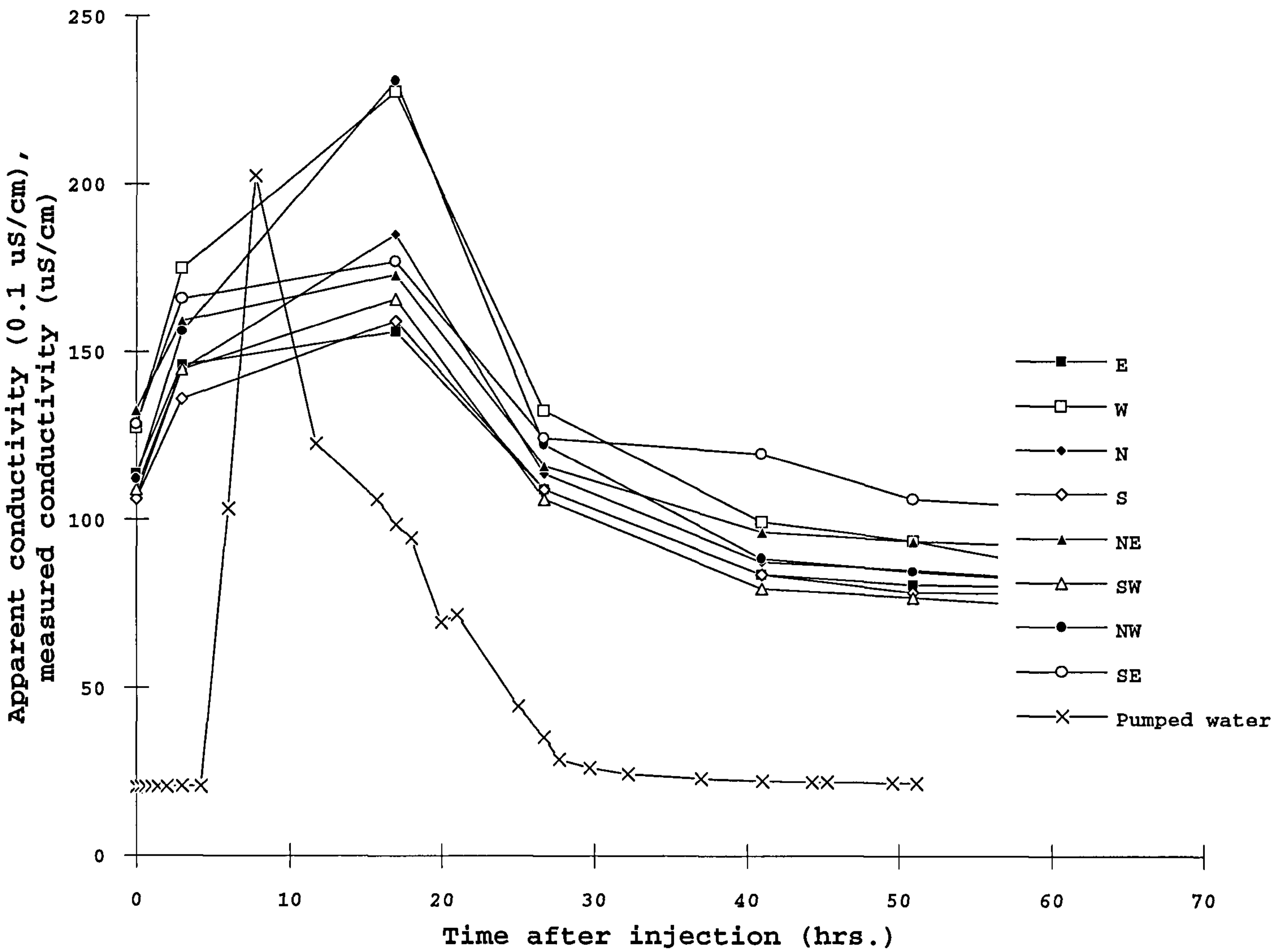

Figure 16. Apparent conductivity from potential measurements for station interval 2-1 and measured conductivity of pumped water.

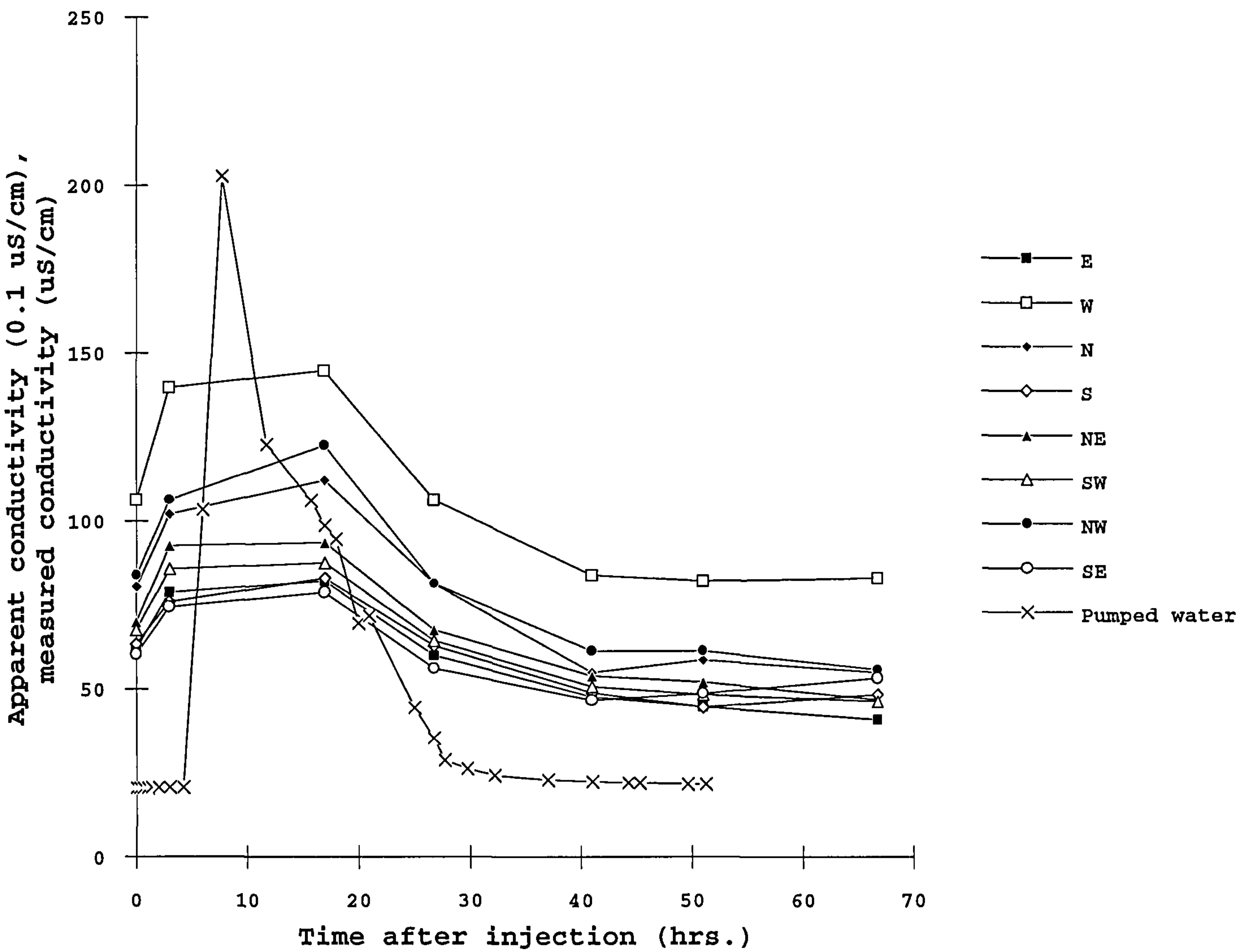

Figure 17. Apparent conductivity from potential measurements for station interval 4-2 and measured conductivity of pumped water.

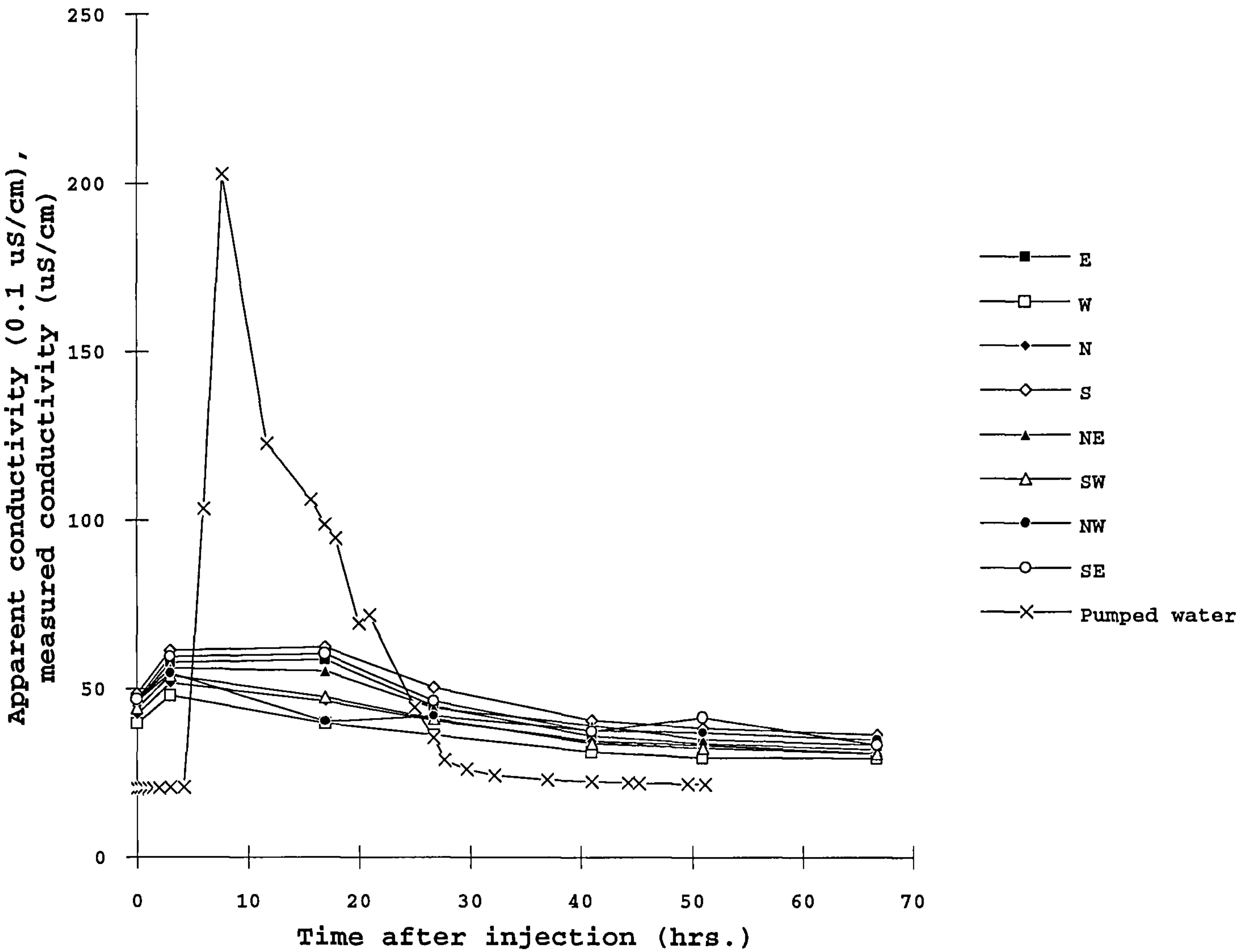

Figure 18. Apparent conductivity from potential measurements for station interval 8-4 and measured conductivity of pumped water.

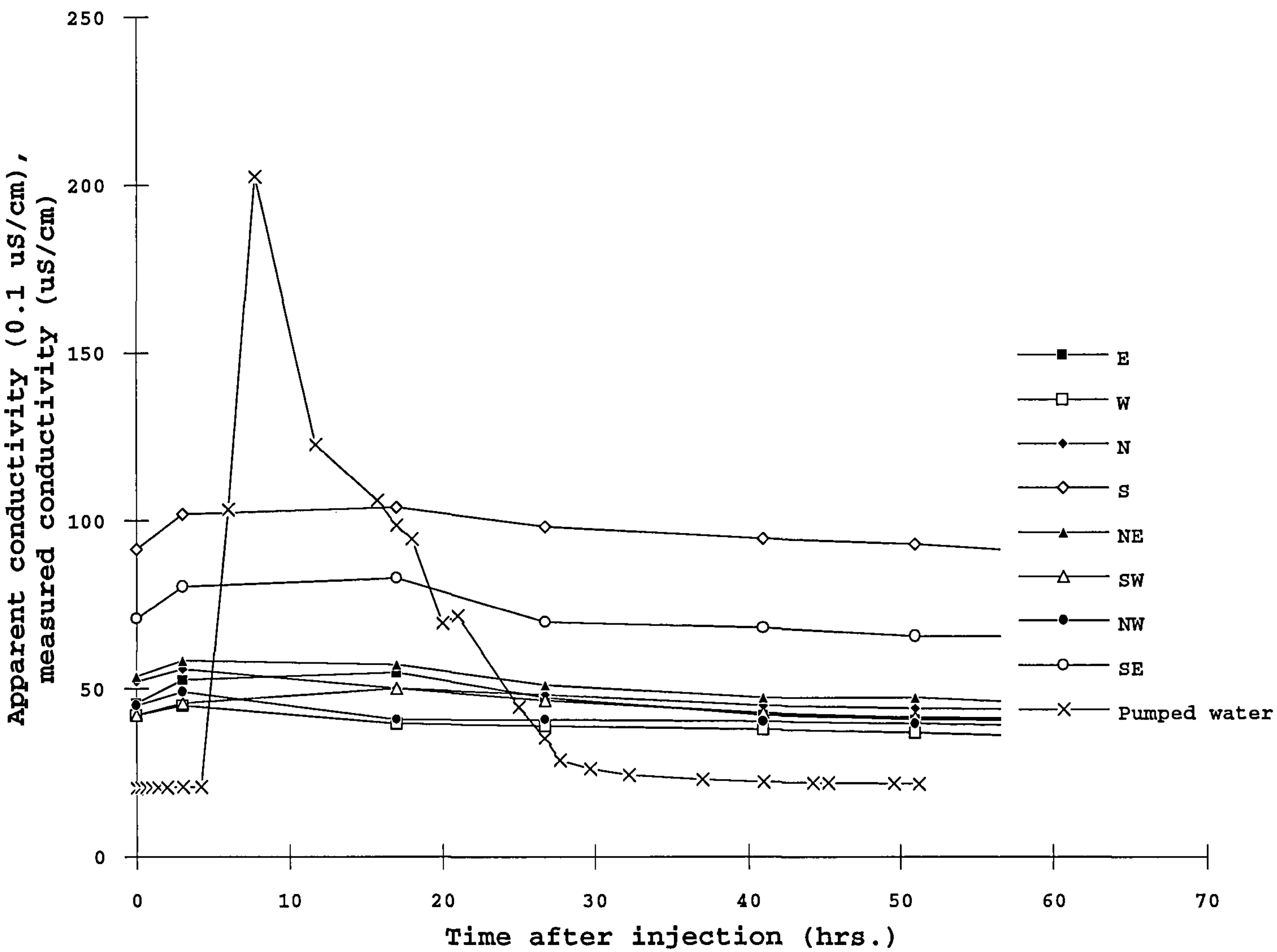

Figure 19. Apparent conductivity from potential measurements for station interval 30-20 and measured conductivity of pumped water.

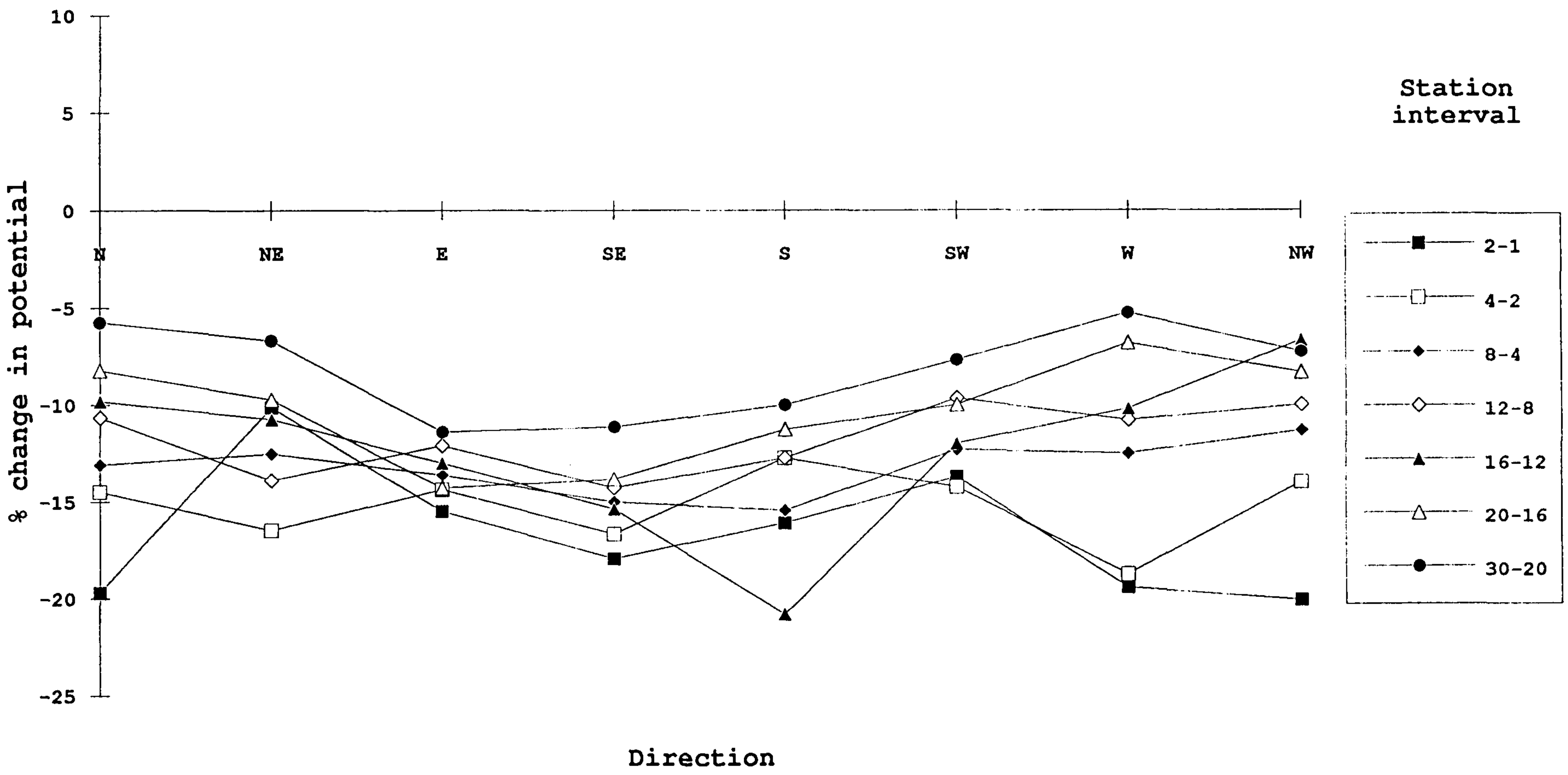

Figure 20. Change in potential from CP1 to CP2 with respect to background (CP7).

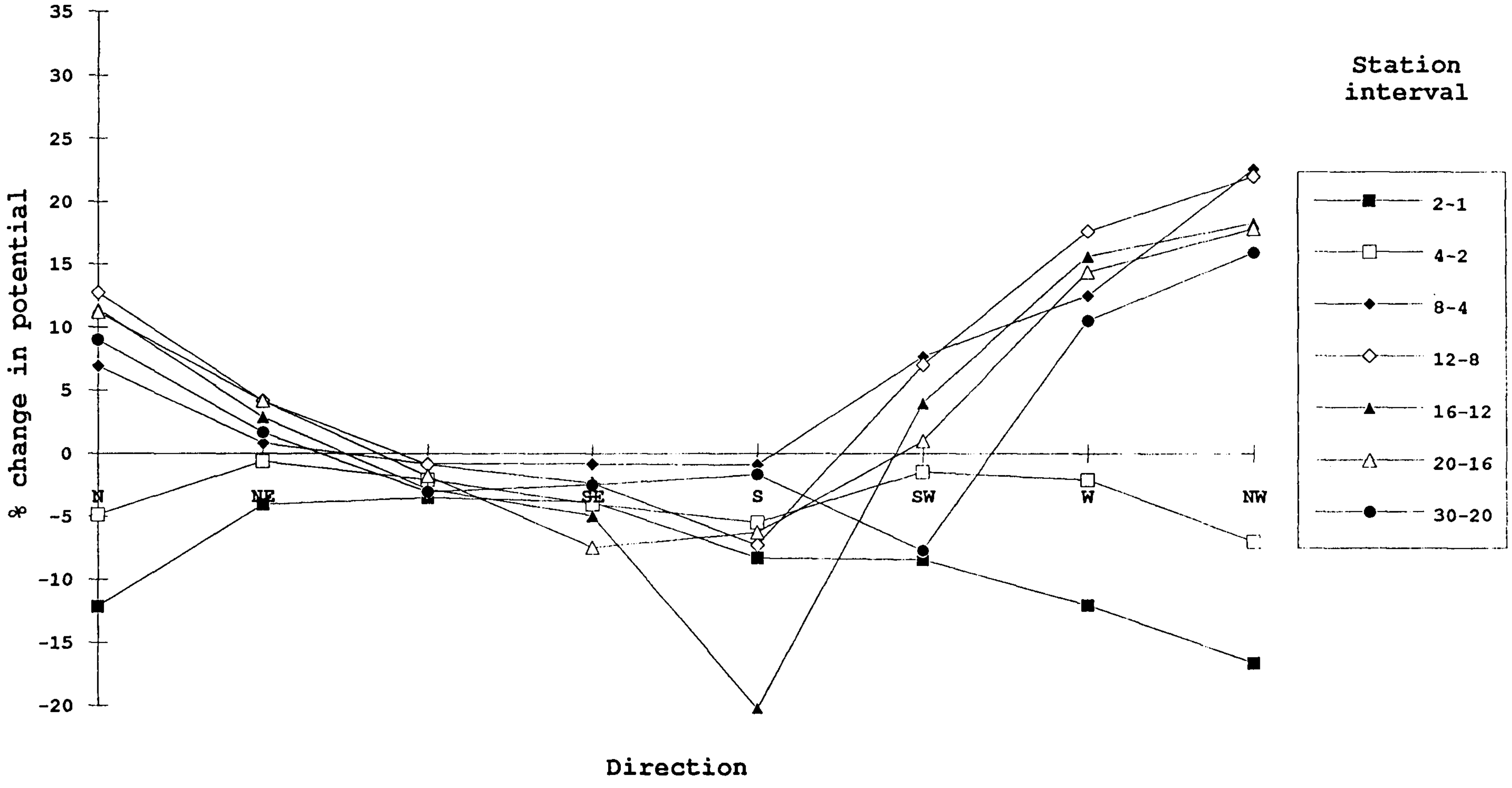

Figure 21. Change in potential from CP2 to CP3 with respect to background (CP7).

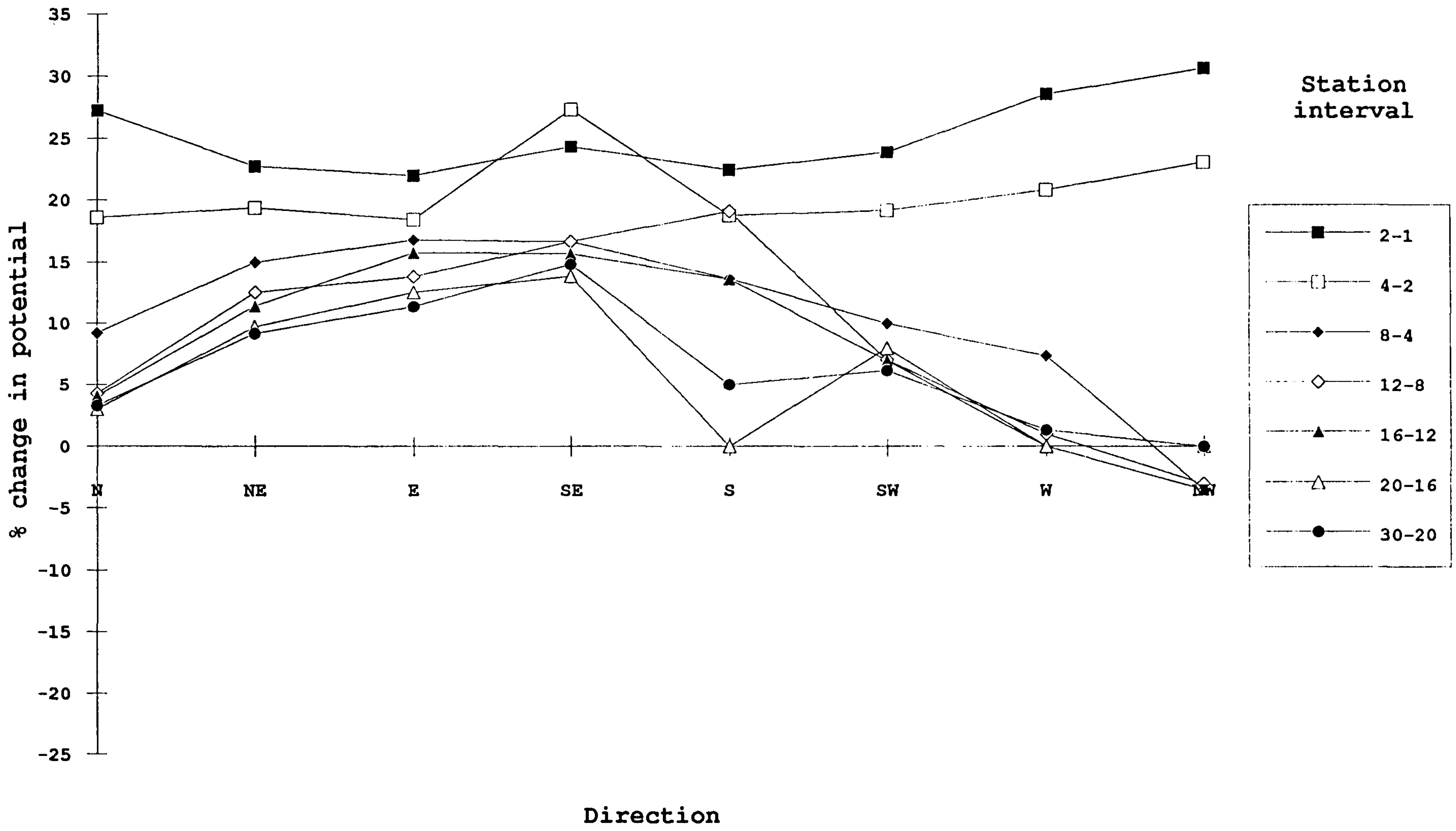

Figure 22. Change in potential from CP3 to CP4 with respect to background (CP7).

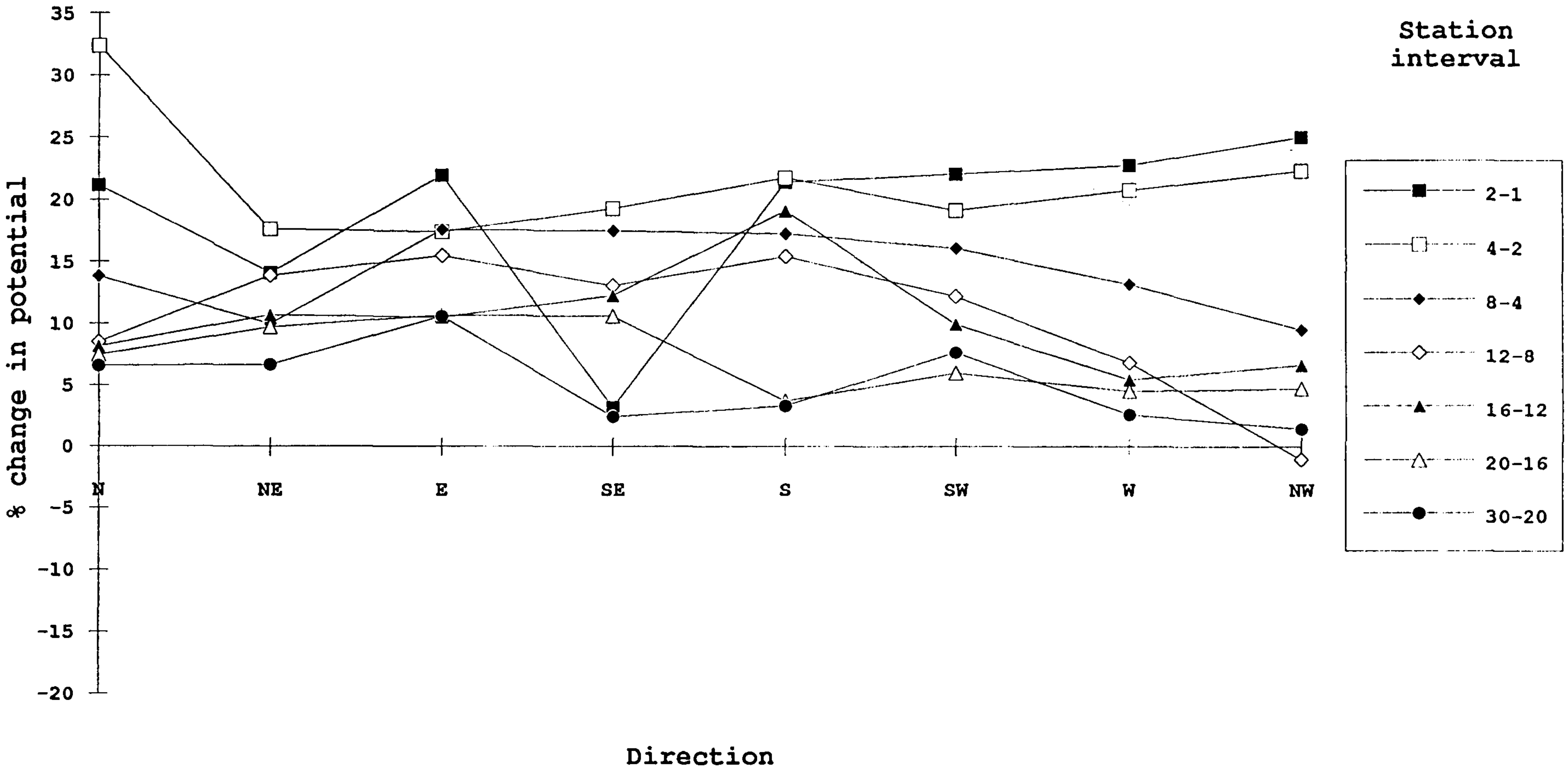

Figure 23. Change in potential from CP4 to CP5 with respect to background (CP7).

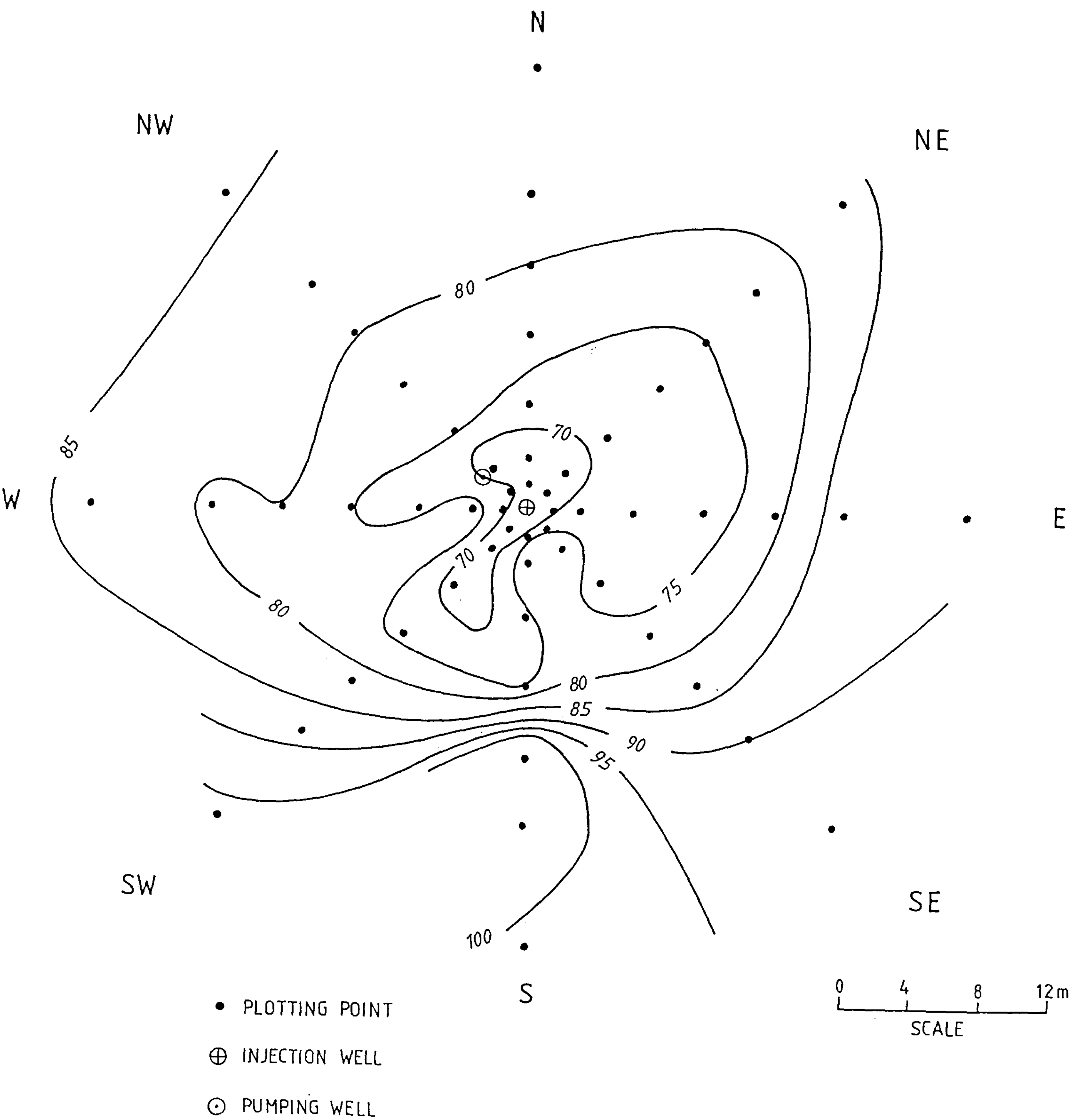

Figure 24. Contour map of ΔCP1/ΔCP7

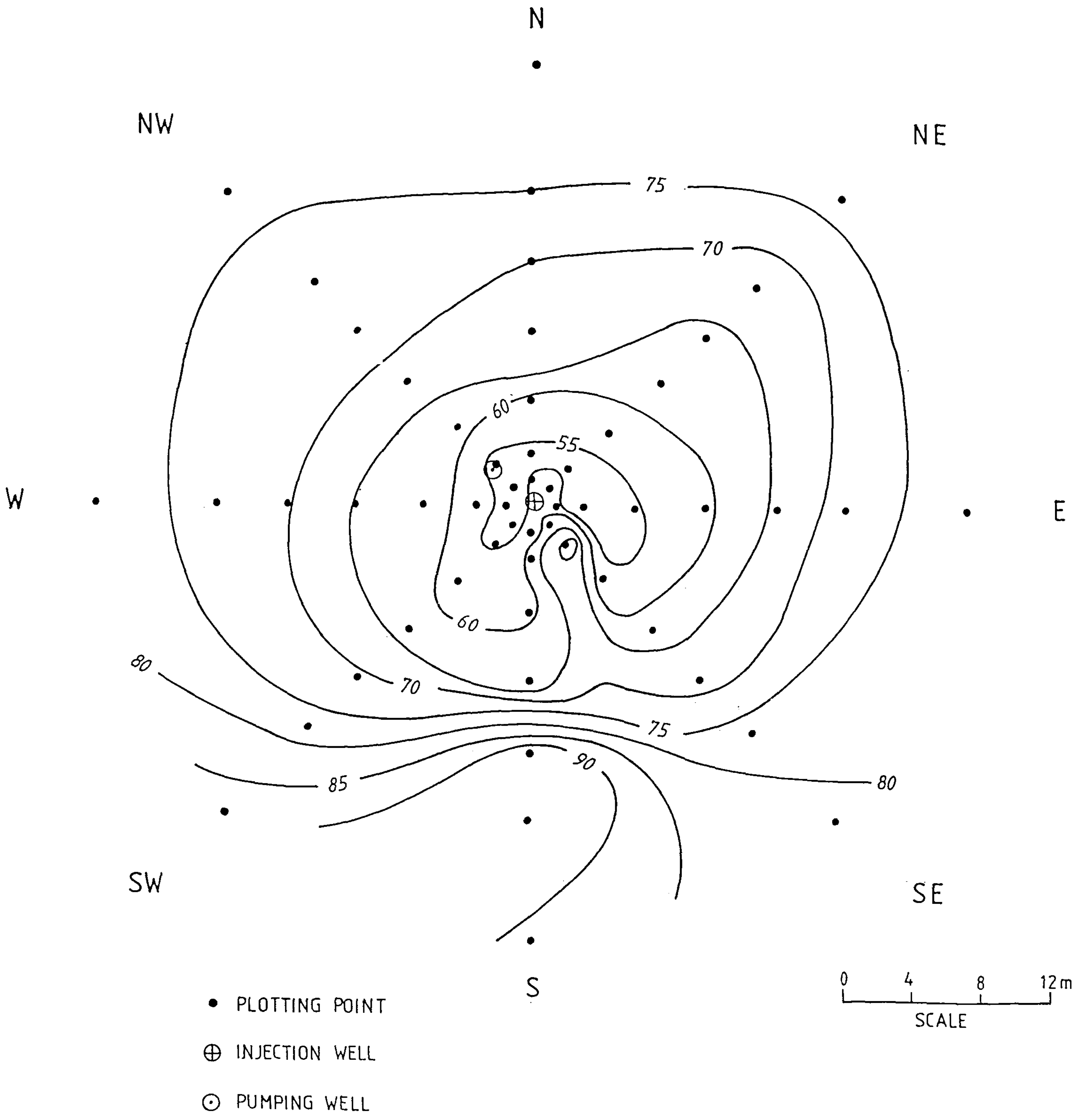

Figure 25. Contour map of $\Delta CP2/\Delta CP7$

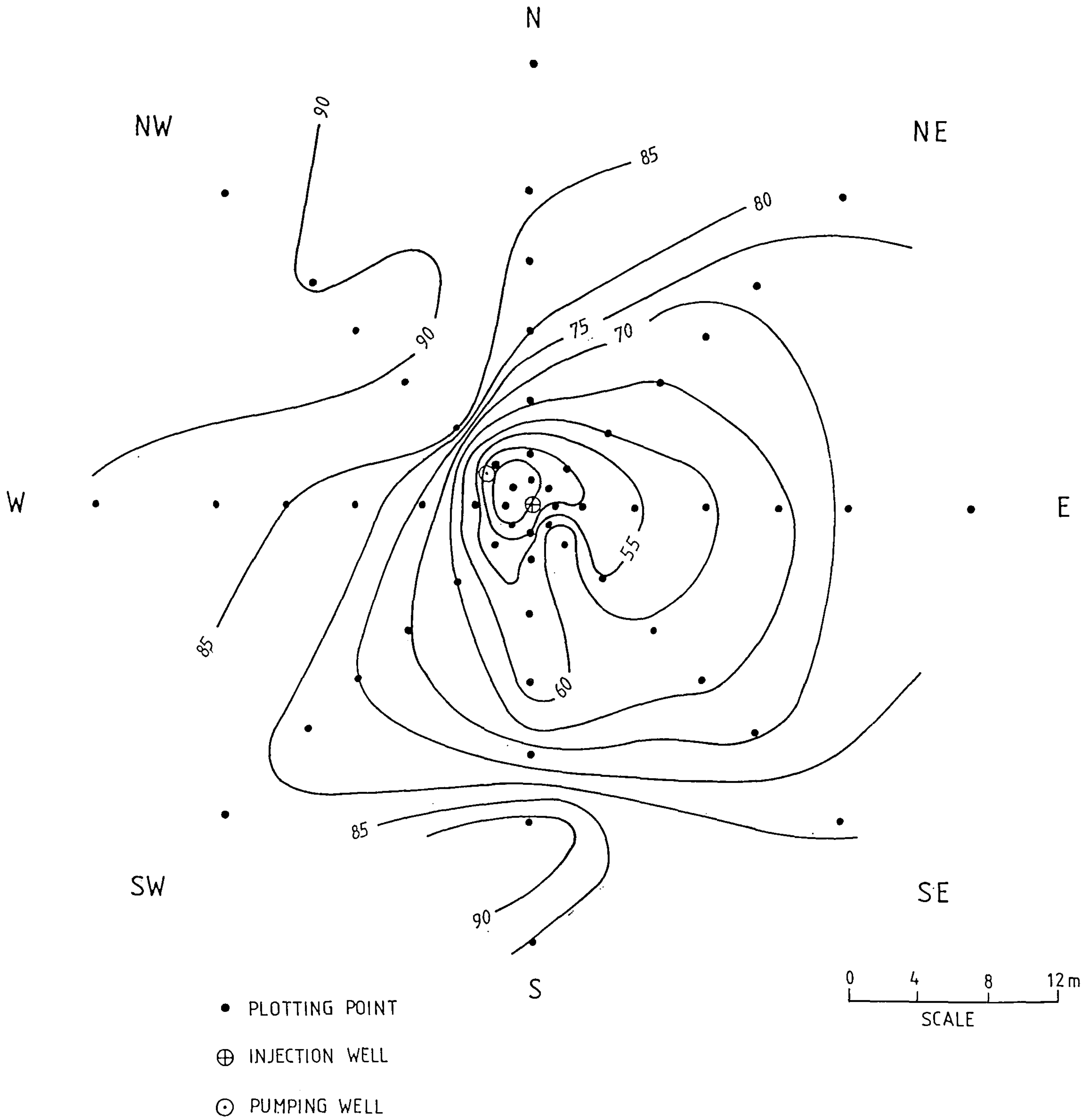

Figure 26. Contour map of ΔCP3/ΔCP7

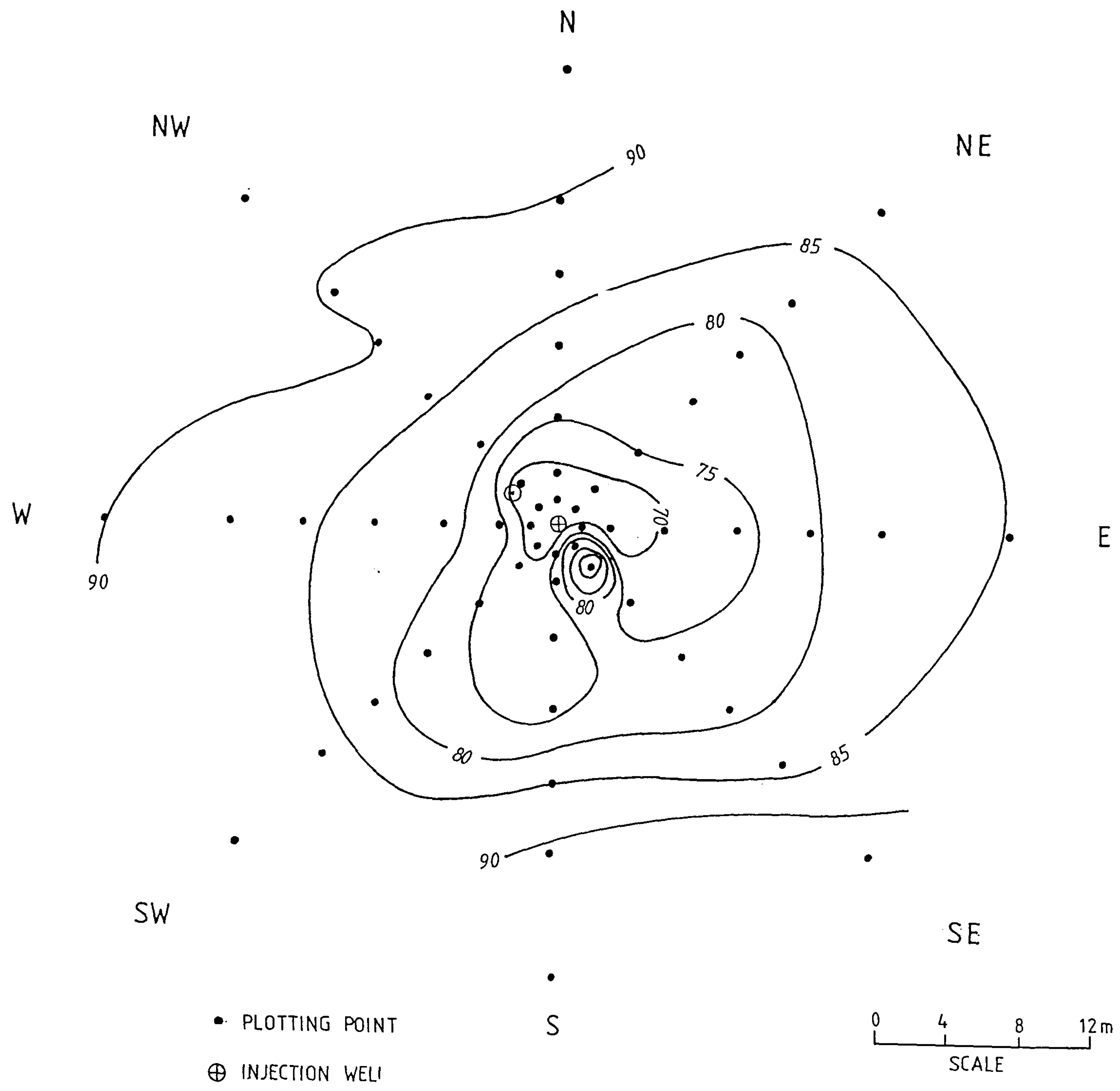

Figure 27. Contour map of ΔCP4/ΔCP7

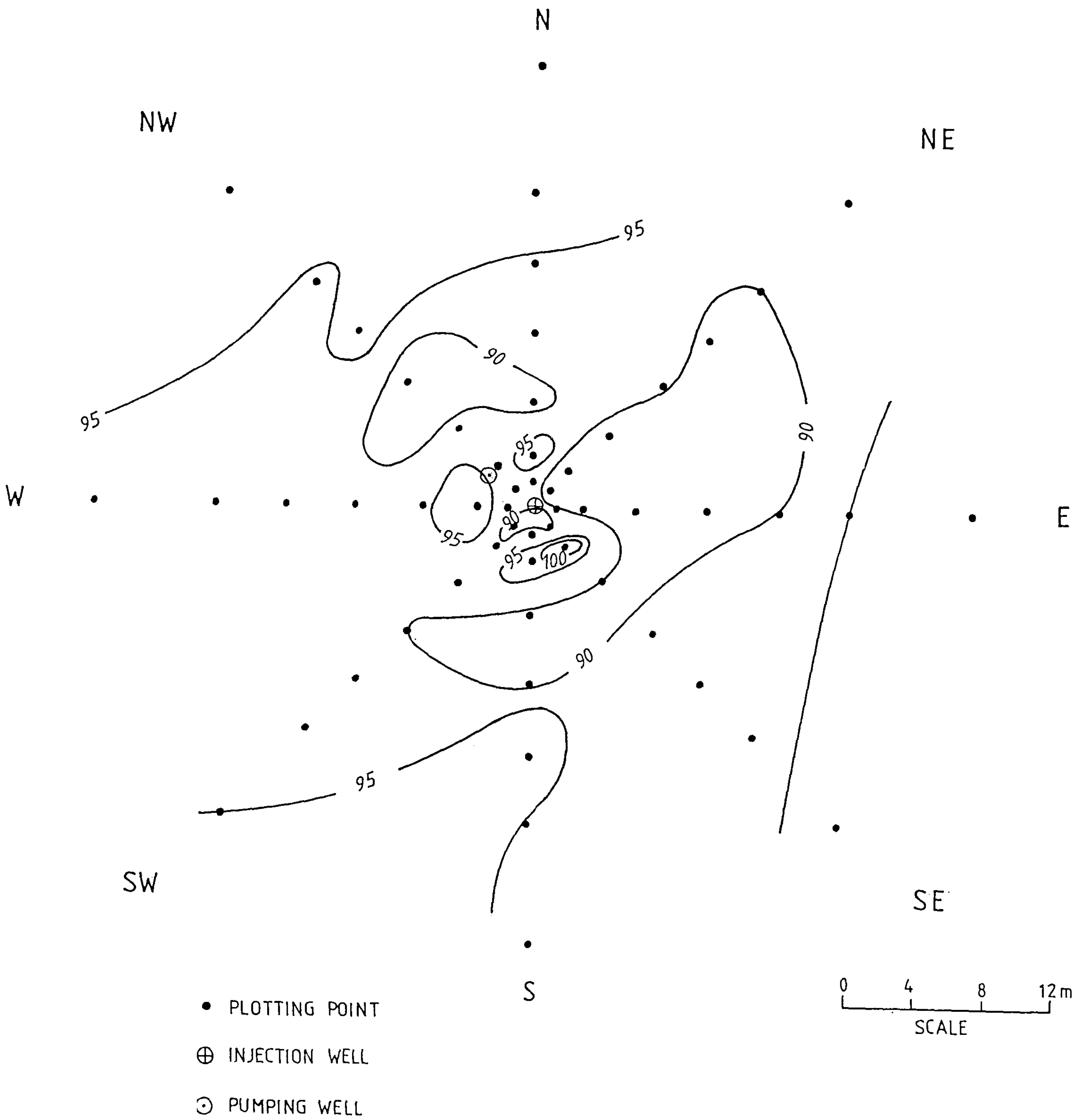

Figure 28. Contour map of ΔCP5/ΔCP7

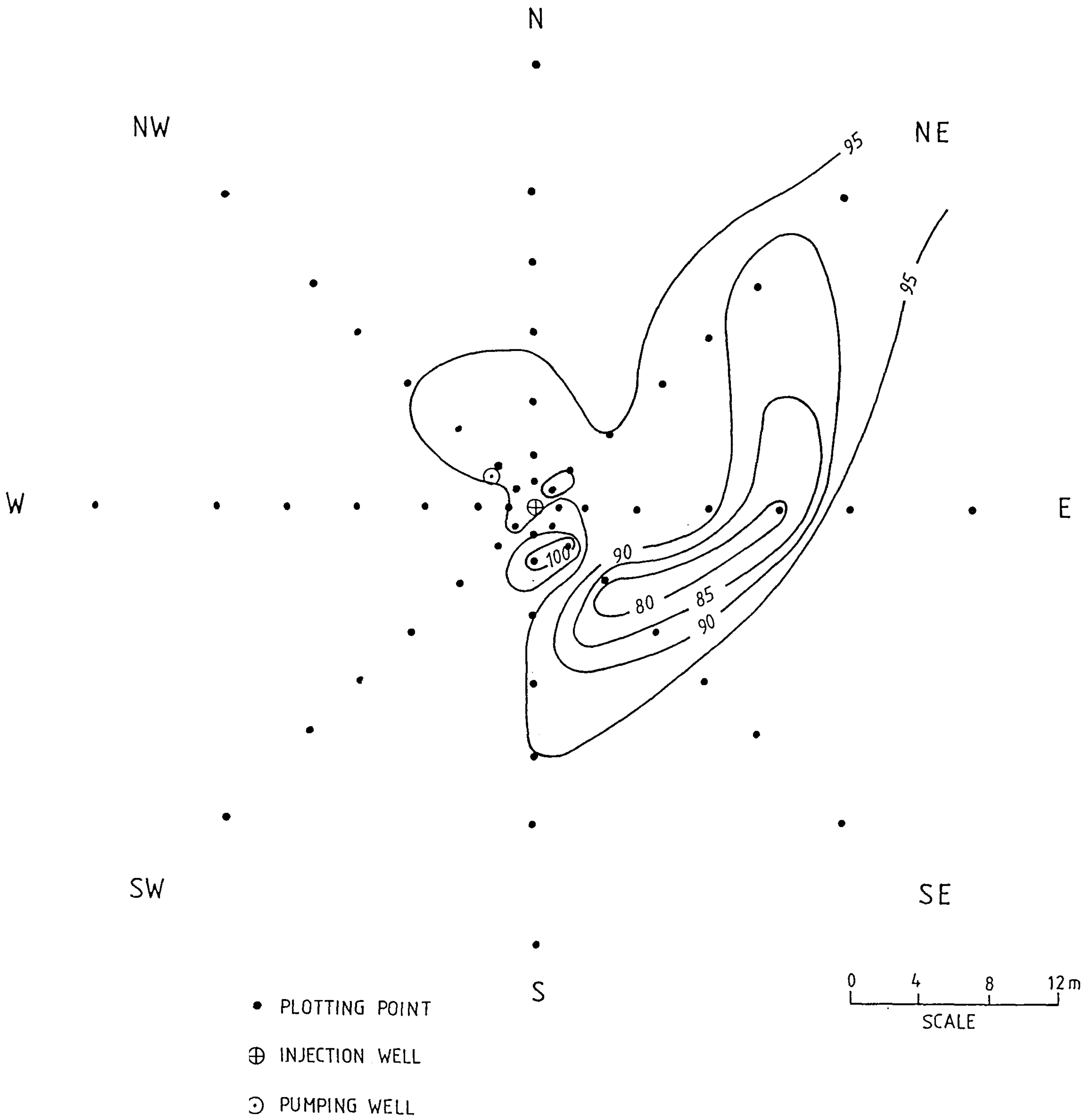

Figure 29. Contour map of ΔCP6/ΔCP7

Appendix

North potential difference measurements							
Station int.	CP1	CP2	CP3	CP4	CP5	CP6	CP7
30-20	1020	950	1060	1100	1180	1200	1220
20-16	1120	1010	1160	1200	1300	1320	1340
16-12	1960	1720	2000	2100	2300	2350	2450
12-8	3650	3150	3750	3950	4350	4500	4700
8-4	9400	7700	8600	9800	11600	12000	13000
4-2	9900	7800	7100	9800	14500	13600	14500
2-1	14900	11000	8600	1400	18200	18700	19800

Northeast potential difference measurements							
Station int.	CP1	CP2	CP3	CP4	CP5	CP6	CP7
30-20	990	910	930	1040	1120	1120	1200
20-16	1100	960	1020	1160	1300	1240	1440
16-12	2100	1800	1880	2200	2500	2600	2800
12-8	2700	2200	2350	2800	3300	3300	3600
8-4	8600	7100	7200	9000	10200	11400	12000
4-2	11400	8600	8500	11800	14800	15300	17000
2-1	12000	10000	9200	13700	16500	17000	19800

East potential difference measurements							
Station int.	CP1	CP2	CP3	CP4	CP5	CP6	CP7
30-20	1160	1010	970	1120	1260	1300	1320
20-16	490	410	400	470	530	560	560
16-12	2250	1880	1800	2250	2550	2250	2850
12-8	4150	3450	3400	4200	5100	5400	5800
8-4	8600	6900	6800	8900	11100	11800	12500
4-2	12900	10100	9700	13300	16700	17800	19500
2-1	14000	10900	10200	14600	19000	19700	20000

Southeast potential difference measurements							
Station int.	CP1	CP2	CP3	CP4	CP5	CP6	CP7
30-20	750	660	640	760	780	810	810
20-16	850	720	650	780	880	920	940
16-12	2700	2200	2040	2550	2950	3200	3250
12-8	3250	2650	2550	3250	3800	3600	4200
8-4	8500	6700	6600	8600	10700	9600	12000
4-2	13200	10700	10100	14200	17100	16400	15000
2-1	12400	9600	9000	12800	13300	15000	15600

South potential difference measurements							
Station int.	CP1	CP2	CP3	CP4	CP5	CP6	CP7
30-20	580	1160	510	540	560	570	600
20-16	870	780	730	730	760	780	800
16-12	2700	2200	1714	2040	2500	2250	2400
12-8	4100	3400	3000	4050	4900	5250	5500
8-4	8200	6500	6400	7900	9800	10400	11000
4-2	12600	10500	9600	12700	16300	17900	16500
2-1	15000	11700	10000	14600	19000	20300	20500

Southwest potential difference measurements							
Station int.	CP1	CP2	CP3	CP4	CP5	CP6	CP7
30-20	1260	1160	1060	1140	1240	1280	1300
20-16	870	770	780	860	920	980	1000
16-12	1660	1420	1000	1640	1840	1900	2000
12-8	4150	3600	4000	4400	5100	5400	5700
8-4	9000	7400	8400	9700	11800	12300	13000
4-2	11800	9300	9100	12400	15700	16500	17200
2-1	14600	11000	9600	15000	20000	20700	22600

West potential difference measurements							
Station int.	CP1	CP2	CP3	CP4	CP5	CP6	CP7
30-20	1260	1180	1340	1360	1400	1440	1520
20-16	1040	950	1140	1140	1200	1280	1320
16-12	2200	1920	2350	2350	2500	2600	2750
12-8	3850	3300	4200	4250	4600	5000	5100
8-4	10000	8300	10000	11000	12800	13500	13600
4-2	7500	5700	5500	7500	9500	9700	9600
2-1	12500	9100	7000	12000	16000	17000	17500

Northwest potential difference measurements							
Station int.	CP1	CP2	CP3	CP4	CP5	CP6	CP7
30-20	1180	1080	1300	1300	1320	1340	1380
20-16	1340	1200	1500	1500	1580	1600	1680
16-12	2400	2200	2750	2700	2900	2900	3000
12-8	3850	3350	4450	4300	4250	4750	5000
8-4	8600	7300	9900	9500	10600	10800	11500
4-2	9500	7500	6500	9800	13000	13000	14300
2-1	14200	10200	6900	1300	18000	18800	19900